LETTER

doi:10.1038/nature09883

BCL6 enables Ph$^+$ acute lymphoblastic leukaemia cells to survive *BCR–ABL1* kinase inhibition

Cihangir Duy[1,2], Christian Hurtz[1,6], Seyedmehdi Shojaee[1], Leandro Cerchietti[3], Huimin Geng[3], Srividya Swaminathan[1], Lars Klemm[1], Soo-mi Kweon[2], Rahul Nahar[1,2], Melanie Braig[4], Eugene Park[2], Yong-mi Kim[2], Wolf-Karsten Hofmann[5], Sebastian Herzog[6], Hassan Jumaa[6], H. Phillip Koeffler[7], J. Jessica Yu[8], Nora Heisterkamp[2], Thomas G. Graeber[9], Hong Wu[9], B. Hilda Ye[8], Ari Melnick[3] & Markus Müschen[1,2]

Tyrosine kinase inhibitors (TKIs) are widely used to treat patients with leukaemia driven by *BCR–ABL1* (ref. 1) and other oncogenic tyrosine kinases[2,3]. Recent efforts have focused on developing more potent TKIs that also inhibit mutant tyrosine kinases[4,5]. However, even effective TKIs typically fail to eradicate leukaemia-initiating cells (LICs)[6–8], which often cause recurrence of leukaemia after initially successful treatment. Here we report the discovery of a novel mechanism of drug resistance, which is based on protective feedback signalling of leukaemia cells in response to treatment with TKI. We identify BCL6 as a central component of this drug-resistance pathway and demonstrate that targeted inhibition of BCL6 leads to eradication of drug-resistant and leukaemia-initiating subclones.

BCL6 is a known proto-oncogene that is often translocated in diffuse large B-cell lymphoma (DLBCL)[9]. In response to TKI treatment, *BCR–ABL1* acute lymphoblastic leukaemia (ALL) cells upregulate BCL6 protein levels by approximately 90-fold: that is, to similar levels as in DLBCL (Fig. 1a). Upregulation of BCL6 in response to TKI treatment represents a novel defence mechanism, which enables leukaemia cells to survive TKI treatment: Previous work suggested that TKI-mediated cell death is largely p53 independent. Here we demonstrate that BCL6 upregulation upon TKI treatment leads to transcriptional inactivation of the p53 pathway. BCL6-deficient leukaemia cells fail to inactivate p53 and are particularly sensitive to TKI treatment. BCL6$^{-/-}$ leukaemia cells are poised to undergo cellular senescence and fail to initiate leukaemia in serial transplant recipients. A combination of TKI treatment and a novel BCL6 peptide inhibitor markedly increased survival of NOD/SCID mice xenografted with patient-derived *BCR–ABL1* ALL cells. We propose that dual targeting of oncogenic tyrosine kinases and BCL6-dependent feedback (Supplementary Fig. 1) represents a novel strategy to eradicate drug-resistant and leukaemia-initiating subclones in tyrosine-kinase-driven leukaemia.

To elucidate mechanisms of TKI resistance in tyrosine-kinase-driven leukaemia, we performed a gene expression analysis including our and published data of TKI-treated leukaemia. We identified *BCL6* as a top-ranking gene in a set of recurrent gene expression changes, some of which are shared with mitogen-activated protein-kinase kinase (MEK) inhibition in BRAF^{V600E} mutant solid tumour cells[10] (Supplementary Figs 2 and 3). TKI-induced upregulation of BCL6 messenger RNA (mRNA) levels was confirmed in multiple leukaemia subtypes carrying oncogenic tyrosine kinases (Supplementary Fig. 2). The BCR–ABL1 kinase, encoded by the Philadelphia chromosome (Ph), represents the most frequent genetic lesion in adult ALL, defines the subtype with a particularly poor prognosis[1,4,5] and was therefore chosen as focus for this study.

To elucidate the regulation of BCL6 in Ph$^+$ ALL, we investigated the JAK2/STAT5 (ref. 11) and PI3K/AKT[12] pathways downstream of BCR–ABL1. We and others have shown that STAT5 suppresses BCL6 in B cells[13–15]. TKI-mediated upregulation of BCL6 was diminished by constitutively active STAT5 (Fig. 1b) and deletion of *STAT5* was sufficient to upregulate BCL6, even in the absence of TKI treatment (Fig. 1c). In agreement with previous work[15], overexpression of FoxO4 induced BCL6 (Fig. 1d). In Ph$^+$ ALL cells, FoxO factors are inactivated by PI3K/AKT[12] signalling, which is reversed by Pten (Supplementary Fig. 4). Deletion of *Pten*, hence, abrogated the ability of the leukaemia cells to upregulate BCL6 in response to TKI treatment (Fig. 1e).

In DLBCL, BCL6 is frequently translocated and suppresses p53-mediated apoptosis[9,16]. Although TKI treatment is less effective in p53$^{-/-}$ Ph$^+$ ALL[17], recent studies showed that TKI paradoxically prevents the upregulation of p53 in response to DNA damage in Ph$^+$ ALL and chronic myelogenous leukaemia[18,19]. A comparative gene expression analysis of BCL6$^{-/-}$ and BCL6$^{+/+}$ ALL cells (Supplementary Fig. 5) identified Cdkn2a (Arf), Cdkn1a (p21), p53 and p53bp1 as potential BCL6 target genes (Supplementary Fig. 6). Arf and p53 protein levels were indeed unrestrained in BCL6$^{-/-}$ ALL (Fig. 2a). TKI treatment of BCL6$^{+/+}$ ALL resulted in strong upregulation of BCL6 with low levels of p53, whereas BCL6$^{-/-}$ ALL cells failed to curb p53 expression levels (Supplementary Fig. 7). Likewise, TKI treatment increased excessively p53 levels when *Pten*-deficient ALL cells failed to upregulate BCL6 (Fig. 1e).

Identifying direct targets of BCL6 by chromatin immunoprecipitation (ChIP) in Ph$^+$ ALL (Supplementary Figs 8–11), p53, p21 and p27 were among the genes with the strongest recruitment of BCL6 in TKI-treated ALL (Fig. 2b and Supplementary Figs 9–11). Given that cell-cycle arrest and senescence-associated genes were among the BCL6 targets, we studied the cell-cycle profile of leukaemia cells. BCL6$^{-/-}$ ALL cells divided at a slightly reduced rate compared with BCL6$^{+/+}$ ALL cells (Fig. 2c). Treatment with adriamycin (0.05 μg ml^{-1}) had no significant effect on BCL6$^{+/+}$ ALL cells in a senescence-associated β-galactosidase assay[20,21] but revealed that most BCL6$^{-/-}$ leukaemia cells were poised to undergo cellular senescence (Fig. 2d). These findings demonstrate that even low levels of BCL6 in the absence of TKI treatment are critical to downregulate Arf/p53.

Clonal evolution of leukaemia involves acquisition of genetic lesions through DNA damage[22]. Interestingly, a comparative genomic hybridization analysis revealed that genetic lesions were less frequent in BCL6 deficient ALL (Supplementary Fig. 12), suggesting that increased sensitivity to DNA damage limits clonal evolution in the absence of BCL6. Because Arf and p53 are critical negative regulators of self-renewal[23], we performed colony-forming assays. The colony frequencies of

[1]Department of Laboratory Medicine, University of California San Francisco, San Francisco, California 94143, USA. [2]Children's Hospital Los Angeles, Department of Pediatrics, University of Southern California, Los Angeles, California 90027, USA. [3]Departments of Medicine and Pharmacology, Weill Cornell Medical College, New York, New York 10065, USA. [4]Department of Hematology and Oncology, Universitätsklinikum Hamburg-Eppendorf, Hamburg, Germany. [5]Department of Hematology and Oncology, Universität Heidelberg, Klinikum Mannheim, Mannheim, Germany. [6]Faculty of Biology, BIOSS Centre for Biological Signalling Studies, Albert-Ludwigs-Universität Freiburg and Max-Planck-Institute for Immunobiology, Freiburg, Germany. [7]Division of Hematology and Oncology, Cedars Sinai Medical Center, Los Angeles, California 90095, USA. [8]Department of Cell Biology, Albert Einstein College of Medicine, Bronx, New York 10461, USA. [9]Department of Molecular Pharmacology, University of California Los Angeles, Los Angeles, California 90095, USA.

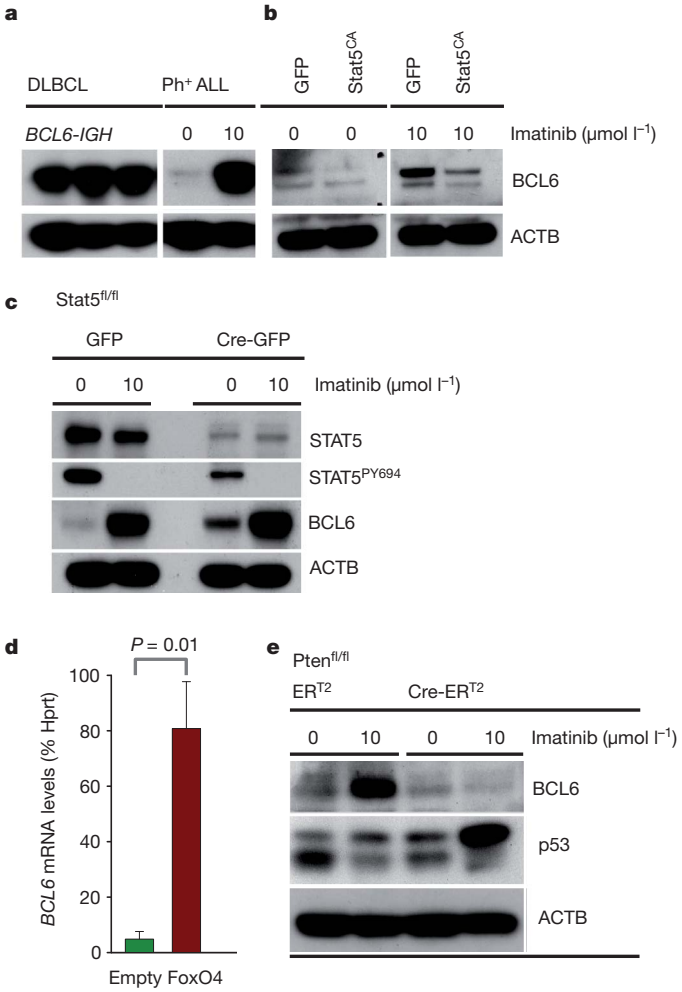

Figure 1 | Regulation of BCL6 expression in BCR–ABL1 ALL cells. **a**, Ph^+ ALL cells were treated with and without imatinib (10 μmol l^{-1}) for 24 h. Upregulation of BCL6 was compared with expression levels in DLBCL by western blot. **b**, *BCR–ABL1*-transformed mouse ALL cells were transduced with a constitutively active Stat5 mutant ($STAT5^{CA}$) or a control vector (green fluorescent protein, GFP) and treated either with or without imatinib. BCL6 western blot was performed using β-actin as loading control. **c**, BCL6 expression upon imatinib treatment was studied by western blot in the presence or absence of Cre-mediated deletion of *Stat5* in *BCR–ABL1*-transformed $Stat5^{fl/fl}$ mouse ALL. **d**, Mouse *BCR–ABL1* ALL cells were transduced with FoxO4-puromycin or a puromycin control vector and subjected to antibiotic selection. Cells were collected and BCL6 mRNA levels were measured by qRT–PCR relative to Hprt. **e**, Imatinib-induced BCL6 expression was studied by western blot in the presence or absence of Cre-mediated deletion of *Pten* in *BCR–ABL1*-transformed $Pten^{fl/fl}$ mouse ALL cells.

$BCL6^{-/-}$ ALL cells were reduced by approximately 20-fold compared with $BCL6^{+/+}$ ALL (Fig. 3a). To study self-renewal *in vivo*, we measured the ability of $BCL6^{+/+}$ and $BCL6^{-/-}$ ALL cells to initiate leukaemia in transplant recipients (Fig. 3b). Using luciferase bioimaging, leukaemia engraftment was observed in both groups after 8 days. $BCL6^{+/+}$ ALL cells rapidly expanded and initiated fatal leukaemia, whereas $BCL6^{-/-}$ ALL cells failed to expand from the initial engraftment foci (Fig. 3c). Some mice that received $BCL6^{-/-}$ ALL cells ultimately succumbed to leukaemia (Fig. 3b). Flow cytometry, however, revealed that the leukaemias in the $BCL6^{-/-}$ group were in fact derived from endogenous $CD45.1^+$ cells of the irradiated recipients and not from the injected $CD45.2^+$ donor ALL cells (Supplementary Fig. 13 and asterisks in Fig. 3b).

Defective leukaemia initiation may be a consequence of impaired homing to the bone marrow niche. Indeed, $BCL6^{-/-}$ ALL cells lack expression of CD44 (Supplementary Fig. 14), which is critical for homing of *BCR–ABL1* LICs to the bone marrow microenvironment[24]. Retroviral reconstitution of CD44 markedly increased homing of $BCL6^{-/-}$ ALL cells to the bone marrow niche, but failed to rescue defective leukaemia initiation (Supplementary Fig. 14).

Using intrafemoral injection to circumvent homing defects, a limiting dilution experiment (Fig. 3d) showed that 5 million $BCL6^{-/-}$ ALL cells compared with only 10^3 $BCL6^{+/+}$ ALL cells were needed to initiate fatal leukaemia. These findings suggest that the frequency of LIC in $BCL6^{-/-}$ ALL (fewer than 1 in 100,000) is reduced by more than 100-fold compared with $BCL6^{+/+}$ ALL (at least 1 in 1,000). An alternative interpretation would be that LICs occur at a similar frequency in $BCL6^{-/-}$ ALL but with reduced self-renewal activity. To address potential 'exhaustion' of LICs, we performed a serial transplantation with ALL cells that gave rise to disease in primary recipients after injection of 5 million ALL cells. From the bone marrow, we isolated $CD19^+$ ALL cells for secondary intrafemoral injection. $BCL6^{-/-}$ leukaemia was not transplantable in secondary recipients (Supplementary Fig. 15). Although these findings do not exclude the possibility that the LIC frequencies are reduced in $BCL6^{-/-}$ ALL, they support the notion of LIC 'exhaustion' after secondary transplantation.

To explore the therapeutic usefulness of pharmacological inhibition of BCL6, we tested a BCL6 inhibitor (*retro-inverso* BCL6 peptide-inhibitor (RI-BPI)), which blocks the repressor activity of BCL6 (ref. 25). Gene expression analysis confirmed that RI-BPI is a selective and potent inhibitor of BCL6 (Supplementary Fig. 16). We investigated the effect of RI-BPI on the self-renewal capacity of primary Ph^+ ALL and the initiation of leukaemia in a mouse xenograft model. Treatment with RI-BPI resulted in a reduction of colony formation and delayed progression of leukaemia. Likewise, treatment of Ph^+ ALL with RI-BPI induced cellular senescence (Supplementary Fig. 17).

We next examined how gene dosage of BCL6 affects responses to TKI. For instance, $Pten^{-/-}$ ALL cells lack the ability to upregulate the p53-repressor BCL6 and are more sensitive to imatinib (Fig. 1e and Supplementary Fig. 18). Dose–response studies in $BCL6^{+/+}$, $BCL6^{+/-}$ and $BCL6^{-/-}$ ALL (Fig. 4a) showed that sensitivity to imatinib was significantly increased in $BCL6^{-/-}$ (half maximal effective concentration (EC_{50}) 0.17 μmol l^{-1}) and even in $BCL6^{+/-}$ ALL cells (EC_{50} 0.67 μmol l^{-1}) compared with $BCL6^{+/+}$ ALL cells (EC_{50} 1.10 μmol l^{-1}; Fig. 4a). These findings indicate that maximum levels of BCL6 expression are required to prevent TKI-induced cell death. Indeed, inducible activation of BCL6-ER^{T2} constructs[26] in $BCL6^{-/-}$ ALL cells conferred a strong survival advantage in the presence of imatinib (Fig. 4b). Activation of BCL6 in $BCL6^{+/+}$ ALL cells induced cell-cycle exit (not shown) and no additional survival advantage, because these cells already achieved maximal upregulation of endogenous BCL6 (Fig. 1a).

To address the role of BCL6-mediated repression of p53 in TKI-resistance, $p53^{-/-}$ and $p53^{+/+}$ ALL cells were treated with RI-BPI. The synergistic effect between TKI treatment and RI-BPI is indeed partly p53 dependent (Supplementary Fig. 19). In $p53^{-/-}$ ALL cells, the effect of RI-BPI was significantly diminished compared with $p53^{+/+}$ ALL.

To confirm that BCL6 has a similar function in patient-derived Ph^+ ALL, primary ALL cells were transduced with a dominant-negative BCL6 mutant (DN-BCL6-ER^{T2})[26], which resulted in a marked competitive disadvantage of Ph^+ ALL cells, that was further enhanced by imatinib treatment (Fig. 4c). Similar observations in mouse ALL and in an established Ph^+ ALL cell line demonstrated that BCL6 promotes survival of TKI-treated Ph^+ ALL (Supplementary Fig. 20).

To test the effect of BCL6 inhibition on TKI resistance, we cultured four primary Ph^+ ALL in the presence or absence of imatinib, RI-BPI or a combination of both (Supplementary Fig. 21). Initially, all four Ph^+ ALL cases responded to imatinib treatment, but subsequently rebounded and were no longer sensitive to imatinib (10 μmol l^{-1}). RI-BPI alone showed only slight effects, whereas the combination of RI-BPI and imatinib rapidly induced cell death and effectively prevented a rebound in all four cases (Supplementary Fig. 21). These

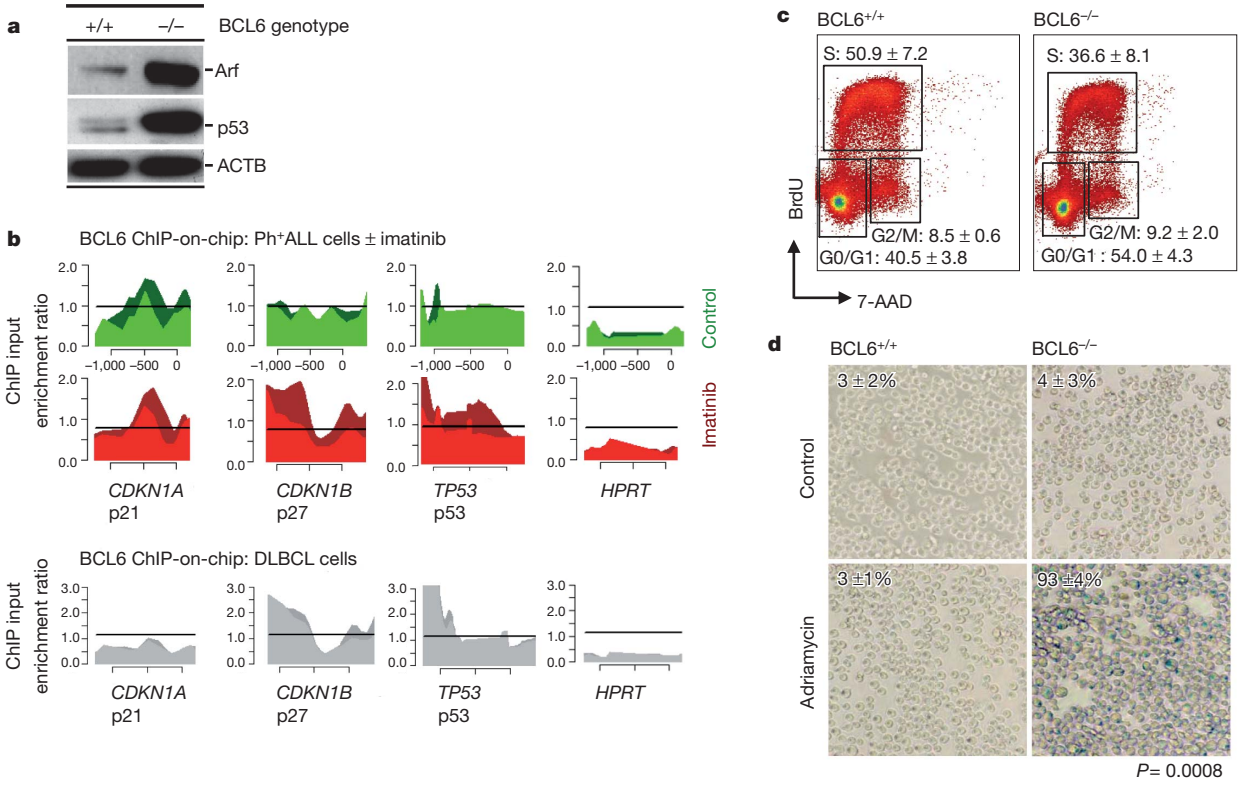

Figure 2 | BCL6 is required for transcriptional inactivation of the Arf/p53 pathway in BCR–ABL1 ALL. **a**, Western blot analysis of CDKN2A (Arf) and p53 expression in BCL6$^{-/-}$ and BCL6$^{+/+}$ *BCR–ABL1* ALL cells. **b**, Human Ph^{+} ALL cells (Tom1) were treated with and without imatinib (10 μmol l^{-1}) for 24 h and were subjected to ChIP-on-chip analysis using a BCL6-specific antibody. The *y* axis indicates enrichment versus input, the *x* axis the location of probes within the respective loci relative to the transcriptional start site. The dark and light green (control) or red (imatinib) tracings depict two replicates. Recruitment to *CDKN1A*, *CDKN1B*, *TP53* and *HPRT* (negative control) is shown in Ph^{+} ALL cells and one DLBCL cell line (OCI-Ly7). **c**, Cell-cycle analysis (BrdU/7-AAD staining). **d**, Staining for senescence-associated β-galactosidase (SA-β-gal). ALL cells were treated with or without 0.05 μg ml^{-1} adriamycin for 48 h to induce a low level of DNA damage. Percentages of SA-β-gal^{+} cells are indicated (means ± SD; $n = 3$).

findings suggest that prolonged treatment with a combination of imatinib/RI-BPI prevents acquisition of TKI-resistance. We next examined the effect of imatinib/RI-BPI combinations on primary TKI-resistance in Ph^{+} ALL. To this end, four human Ph^{+} ALL cell lines that lacked *BCR–ABL1* kinase mutations (Supplementary Table 1) but which were highly refractory to imatinib (10 μmol l^{-1}) were treated with or without imatinib, RI-BPI or a combination of both. Imatinib alone did not achieve a therapeutic response, whereas the combination with RI-BPI potentiated the effect of imatinib on the refractory ALL cells (Supplementary Fig. 22).

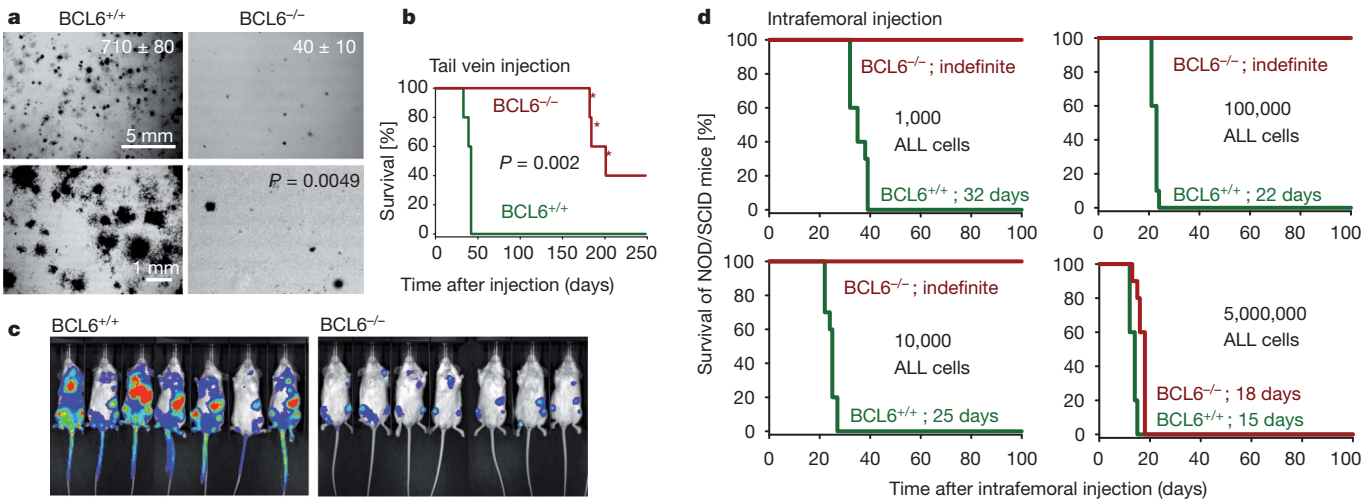

Figure 3 | BCL6 is required for leukaemia initiation in BCR–ABL1 ALL. **a**, Ten thousand BCL6$^{-/-}$ or BCL6$^{+/+}$ *BCR–ABL1* ALL cells were plated in semisolid agar, and colonies were counted after 10 days (numbers denote means ± SD, $n = 3$). **b**, Overall survival of mice injected with 100,000 BCL6$^{-/-}$ and BCL6$^{+/+}$ *BCR–ABL1* ALL cells was compared by Kaplan–Meier analysis. Mice that developed CD45.1^{+} endogenous leukaemia instead of leukaemia from injected CD45.2^{+} cells are indicated by asterisks (see Supplementary Fig. 13). **c**, For an SCID LIC (SL-IC) experiment, BCL6$^{-/-}$ and BCL6$^{+/+}$ *BCR–ABL1* ALL cells were labelled with firefly luciferase and intravenously injected into sublethally irradiated NOD/SCID mice. **d**, The SL-IC assay was repeated as a limiting dilution experiment (10^{3}, 10^{4}, 10^{5}, 5 million cells) and leukaemia cells were directly injected into the femoral bone marrow to circumvent potential engraftment defects.

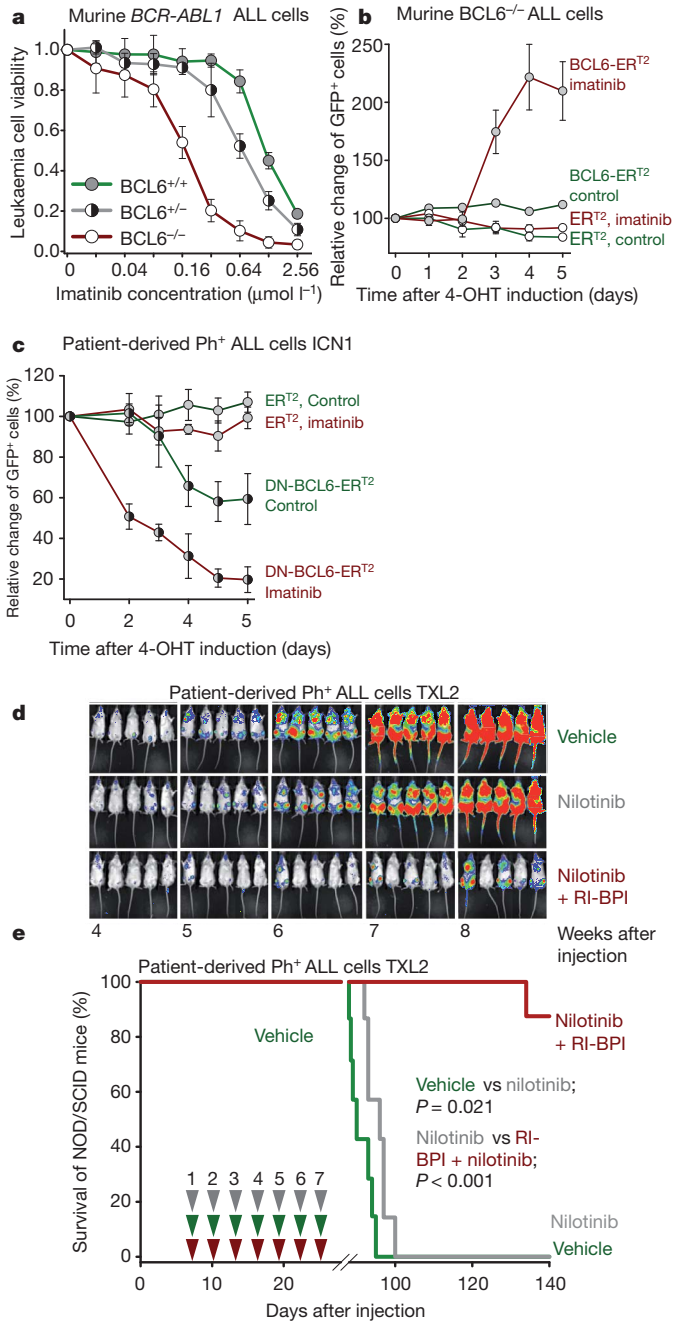

Figure 4 | BCL6 promotes survival of TKI-treated BCR–ABL1 ALL cells. **a**, Imatinib sensitivity of BCL6$^{-/-}$, BCL6$^{+/-}$ and BCL6$^{+/+}$ ALL cells was measured in a resazurin viability assay. **b**, BCL6$^{-/-}$ ALL cells were transduced with BCL6-ER^{T2} or ER^{T2} vectors (tagged with GFP). ALL cells were treated with or without 1 μmol l^{-1} imatinib, and BCL6-ER^{T2} or ER^{T2} were induced by 4-hydroxytamoxifen. Relative changes of GFP^{+} cells after induction are indicated. **c**, Patient-derived Ph^{+} ALL cells (ICN1) were transduced with inducible dominant-negative BCL6 (DN-BCL6-ER^{T2}) or ER^{T2} control vectors. ALL cells were treated with or without 10 μmol l^{-1} imatinib and DN-BCL6-ER^{T2} or ER^{T2} were induced by 4-hydroxytamoxifen. Relative changes of GFP^{+} cells after induction are indicated. **d**, Patient-derived Ph^{+} ALL cells (TXL2) were labelled with luciferase and 100,000 cells were injected. Mice were treated seven times with either vehicle (green), nilotinib (25 mg kg^{-1}; grey) or a combination of nilotinib and RI-BPI (25 mg kg^{-1}; red). Treated mice are shown in **e**, a Kaplan–Meier survival analysis. Treatment days are indicated by arrowheads.

To study the efficacy of combined tyrosine kinase and BCL6 inhibition *in vivo*, primary Ph^{+} ALL cells were labelled with luciferase and xenografted into mice. Recipient mice were treated with either vehicle, nilotinib or a combination of nilotinib and RI-BPI. Nilotinib is more potent than imatinib, which only has marginal effects in mice[27,28]. Bioimaging demonstrated that seven to ten injections of RI-BPI significantly enhanced the effect of nilotinib (Fig. 4d, e and Supplementary Fig. 23). Whereas all mice treated with nilotinib alone succumbed to leukaemia within 99 days after injection, seven of eight mice treated with RI-BPI/nilotinib combination were still alive after 140 days (Fig. 4d, e). Also, in a model for full-blown mouse leukaemia, TKI/RI-BPI combinations proved effective and significantly prolonged survival (Supplementary Fig. 24). Establishing a potential therapeutic window of nilotinib/RI-BPI combinations, we found no evidence of relevant toxicity (Supplementary Figs 25 and 26 and Supplementary Table 2).

Although transcription factors have been considered intractable therapeutic targets, the recent development of a small molecule inhibitor against BCL6 (ref. 29) holds promise for effectively targeting TKI-resistance in patients with Ph^{+} ALL. Because TKI-resistance develops in virtually all cases of Ph^{+} ALL, it appears particularly important to target this novel pathway of TKI-resistance.

METHODS SUMMARY

Cell culture. Primary leukaemia cells (Supplementary Table 1) were cultured on OP9 stroma cells in alpha minimum essential medium without ribonucleotides and deoxyribonucleotides, supplemented with 20% FBS, 2 mM L-glutamine, 1 mM sodium pyruvate, 100 IU ml^{-1} penicillin and 100 μg ml^{-1} streptomycin. Human ALL cell lines were maintained in RPMI with GlutaMAX containing 20% FBS, 100 IU ml^{-1} penicillin and 100 μg ml^{-1} streptomycin. Mouse *BCR–ABL1*-transformed ALL cells were maintained in IMDM with GlutaMAX containing 20% FBS, 100 IU ml^{-1} penicillin, 100 μg ml^{-1} streptomycin and 50 μM 2-mercaptoethanol. Cell cultures were kept at 37 °C in a humidified incubator under a 5% CO_2 atmosphere.

BCR–ABL1 transformation. Transfection of a murine stem cell virus (MSCV)-based retroviral vector encoding BCR–ABL1 was performed using Lipofectamine 2000. Retroviral supernatant was produced by co-transfecting 293FT cells with the plasmids pHIT60 and pHIT123. Virus supernatant was collected, filtered through a 0.45 μm filter and loaded by centrifugation (2,000*g*, 90 min at 32 °C) on 50 μg ml^{-1} RetroNectin-coated non-tissue well plates. Extracted bone marrow cells from mice were transduced by *BCR–ABL1* in the presence of 10 ng ml^{-1} recombinant murine interleukin-7 in RetroNectin-coated Petri dishes.

Full Methods and any associated references are available in the online version of the paper at www.nature.com/nature.

Received 1 February 2010; accepted 31 January 2011.

1. Druker, B. J. *et al.* Activity of a specific inhibitor of the BCR-ABL tyrosine kinase in the blast crisis of chronic myeloid leukemia and acute lymphoblastic leukemia with the Philadelphia chromosome. *N. Engl. J. Med.* **344,** 1038–1042 (2001).
2. Armstrong, S. A. *et al.* Inhibition of FLT3 in MLL. Validation of a therapeutic target identified by gene expression based classification. *Cancer Cell* **3,** 173–183 (2003).
3. Meydan, N. *et al.* Inhibition of acute lymphoblastic leukaemia by a Jak-2 inhibitor. *Nature* **379,** 645–648 (1996).
4. Shah, N. P. *et al.* Overriding imatinib resistance with a novel ABL kinase inhibitor. *Science* **305,** 399–401 (2004).
5. O'Hare, T. *et al.* AP24534, a pan-BCR-ABL inhibitor for chronic myeloid leukemia, potently inhibits the T315I mutant and overcomes mutation-based resistance. *Cancer Cell* **16,** 401–412 (2009).
6. Graham, S. M. *et al.* Primitive, quiescent, Philadelphia-positive stem cells from patients with chronic myeloid leukemia are insensitive to STI571 *in vitro*. *Blood* **99,** 319–325 (2002).
7. Naka, K. *et al.* TGF-β-FOXO signalling maintains leukaemia-initiating cells in chronic myeloid leukaemia. *Nature* **463,** 676–680 (2010).
8. Oravecz-Wilson, K. I. *et al.* Persistence of leukemia-initiating cells in a conditional knockin model of an imatinib-responsive myeloproliferative disorder. *Cancer Cell* **16,** 137–148 (2009).
9. Saito, M. *et al.* A signaling pathway mediating downregulation of BCL6 in germinal center B cells is blocked by BCL6 gene alterations in B cell lymphoma. *Cancer Cell* **12,** 280–292 (2007).
10. Pratilas, C. A. *et al.* (V600E)BRAF is associated with disabled feedback inhibition of RAF-MEK signaling and elevated transcriptional output of the pathway. *Proc. Natl Acad. Sci. USA* **106,** 4519–4524 (2009).

11. Choudhary, C. *et al.* Mislocalized activation of oncogenic RTKs switches downstream signaling outcomes. *Mol. Cell* **36,** 326–339 (2009).
12. Janes, M. R. *et al.* Effective and selective targeting of leukemia cells using a TORC1/2 kinase inhibitor. *Nature Med.* **16,** 205–213 (2010).
13. Walker, S. R., Nelson, E. A. & Frank, D. A. STAT5 represses BCL6 expression by binding to a regulatory region frequently mutated in lymphomas. *Oncogene* **26,** 224–233 (2007).
14. Duy, C. *et al.* BCL6 is critical for the development of a diverse primary B cell repertoire. *J. Exp. Med.* **207,** 1209–1221 (2010).
15. Fernandez de Mattos, S. *et al.* FoxO3a and BCR-ABL regulate cyclin D2 transcription through a STAT5/BCL6-dependent mechanism. *Mol. Cell. Biol.* **24,** 10058–10071 (2004).
16. Phan, R. T. & Dalla-Favera, R. The BCL6 proto-oncogene suppresses p53 expression in germinal-centre B cells. *Nature* **432,** 635–639 (2004).
17. Wendel, H. G. *et al.* Loss of p53 impedes the antileukemic response to BCR-ABL inhibition. *Proc. Natl Acad. Sci. USA* **103,** 7444–7449 (2006).
18. Goldberg, Z., Levav, Y., Krichevsky, S., Fibach, E. & Haupt, Y. Treatment of chronic myeloid leukemia cells with imatinib (STI571) impairs p53 accumulation in response to DNA damage. *Cell Cycle* **3,** 1188–1195 (2004).
19. Skorta, I. *et al.* Imatinib mesylate induces cisplatin hypersensitivity in Bcr-Abl+ cells by differential modulation of p53 transcriptional and proapoptotic activity. *Cancer Res.* **69,** 9337–9345 (2009).
20. Kamijo, T. *et al.* Tumor suppression at the mouse INK4a locus mediated by the alternative reading frame product p19ARF. *Cell* **91,** 649–659 (1997).
21. Braig, M. *et al.* Oncogene-induced senescence as an initial barrier in lymphoma development. *Nature* **436,** 660–665 (2005).
22. Mullighan, C. G. *et al.* Genomic analysis of the clonal origins of relapsed acute lymphoblastic leukemia. *Science* **322,** 1377–1380 (2008).
23. Williams, R. T., Roussel, M. F. & Sherr, C. J. Arf gene loss enhances oncogenicity and limits imatinib response in mouse models of Bcr-Abl-induced acute lymphoblastic leukemia. *Proc. Natl Acad. Sci. USA* **103,** 6688–6693 (2006).
24. Krause, D. S., Lazarides, K., von Andrian, U. H. & Van Etten, R. A. Requirement for CD44 in homing and engraftment of BCR-ABL-expressing leukemic stem cells. *Nature Med.* **12,** 1175–1180 (2006).
25. Cerchietti, L. C. *et al.* A peptomimetic inhibitor of BCL6 with potent antilymphoma effects *in vitro* and *in vivo*. *Blood* **113,** 3397–3405 (2009).
26. Shaffer, A. L. *et al.* BCL-6 represses genes that function in lymphocyte differentiation, inflammation, and cell cycle control. *Immunity* **13,** 199–212 (2000).
27. Williams, R. T. den, B. W. & Sherr, C. J. Cytokine-dependent imatinib resistance in mouse BCR-ABL+, Arf-null lymphoblastic leukemia. *Genes Dev.* **21,** 2283–2287 (2007).
28. Gruber, T. A., Chang, M. S., Sposto, R. & Muschen, M. Activation-induced cytidine deaminase accelerates clonal evolution in BCR-ABL1-driven B-cell lineage acute lymphoblastic leukemia. *Cancer Res.* **70,** 7411–7420 (2010).
29. Cerchietti, L. C. *et al.* A small-molecule inhibitor of BCL6 kills DLBCL cells *in vitro* and *in vivo*. *Cancer Cell* **17,** 400–411 (2010).

Supplementary Information is linked to the online version of the paper at www.nature.com/nature.

Acknowledgements We thank R. Dalla-Favera and L. Hennighausen for sharing $BCL6^{-/-}$ and $STAT5^{fl/fl}$ mice and wild-type controls with us. We thank A. L. Shaffer and L. M. Staudt for sharing their inducible BCL6 constructs. This work was supported by grants from the National Institutes of Health/National Cancer Institute through R01CA104348 (to A.M.), R01CA085573 (to B.H.Y.), R01CA026038 (to H.P.K.), R01CA090321 (to N.H.), R01CA137060 (to M.M.), R01CA139032 (to M.M.), R01CA157664 (to M.M.) and R21CA152497 (to M.M.), grants from the Leukemia and Lymphoma Society (to M.M.) Leukemia and Lymphoma Society SCOR 7005-11 (PI B. J. Druker), a grant from the Alex's Lemonade Stand Foundation for Pediatric Cancer Research (to M.M.), the California Institute for Regenerative Medicine through TR02-1816 (to M.M.), the William Laurence and Blanche Hughes Foundation and a Stand Up To Cancer-American Association for Cancer Research Innovative Research Grant IRG00909 (to M.M.). A.M. and M.M. are Scholars of the Leukemia and Lymphoma Society.

Author Contributions C.D. and M.M. conceived the study and wrote the paper. M.M. and A.M. designed experiments and interpreted data. C.D., C.H., S. Shojaee, L.C., S. Swaminathan, L.K., S.-m.K, R.N., M.B., E.P. and Y.-m.K. designed and performed experiments and interpreted data. W.-K.H., H.P.K. and N.H. provided and characterized samples from patients. H.G. and T.G.G. analysed data. S.H., H.J., J.J.Y., H.W. and B.H.Y. provided important reagents and mouse samples.

Author Information The gene expression and ChIP data are deposited in NCBI's Gene Expression Omnibus under accession numbers GSE23743, GSE24426, GSE15179, GSE11794, GSE10086, GSE20987 and GSE24400. Reprints and permissions information is available at www.nature.com/reprints. The authors declare no competing financial interests. Readers are welcome to comment on the online version of this article at www.nature.com/nature. Correspondence and requests for materials should be addressed to M.M. (markus.muschen@ucsf.edu).

METHODS

Patient samples, human cells and cell lines. Patient samples (Supplementary Table 1) were provided from the departments of Hematology and Oncology, University Hospital Benjamin Franklin, Berlin, Germany (W.-K.H.) and the USC Norris Comprehensive Cancer Center in compliance with Institutional Review Board regulations (approval from the Ethik-Kommission of the Charité, Campus Benjamin Franklin and the IRB of the University of Southern California Health Sciences Campus). Leukaemia cells from bone marrow biopsy of patients with Ph^+ ALL were xenografted into sublethally irradiated NOD/SCID mice by tail vein injection. After passaging, leukaemia cells were collected and cultured on OP9 stroma cells in alpha minimum essential medium (Alpha-MEM, Invitrogen) without ribonucleotides and deoxyribonucleotides, supplemented with 20% fetal bovine serum, 2 mmol l^{-1} L-glutamine, 1 mmol l^{-1} sodium pyruvate, 100 IU ml^{-1} penicillin and 100 μg ml^{-1} streptomycin. The human ALL cell lines BV173, NALM-1, SUP-B15 and TOM1 (obtained from Deutsche Sammlung von Microorganismen und Zellkulturen (DSMZ)) were maintained in Roswell Park Memorial Institute medium (RPMI-1640, Invitrogen) with GlutaMAX containing 20% fetal bovine serum, 100 IU ml^{-1} penicillin and 100 μg ml^{-1} streptomycin.

Retroviral constructs and transduction. Transfection of retroviral constructs encoding BCR–ABL1-IRES-GFP[30], BCR–ABL1-IRES-Neo, STAT5-CA[31], CD44S-Puro[32], FoxO4-Puro, BCL6-ER^{T2}-GFP[26], ER^{T2}-GFP, DN-BCL6-ER^{T2}-GFP, Cre-ER^{T2}-Puro[33], Cre-IRES-GFP, Puro-, Neo- and GFP-empty vector controls were performed using Lipofectamine 2000 (Invitrogen) with Opti-MEM media (Invitrogen). Retroviral supernatant was produced by co-transfecting HEK 293FT cells with the plasmids pHIT60 (ref. 34) (gag-pol) and pHIT123 (ecotropic env) or pHIT456 (amphotropic env). 293FT cells were cultured in high glucose Dulbecco's modified Eagle's medium (DMEM, Invitrogen) with GlutaMAX containing 10% fetal bovine serum, 100 IU ml^{-1} penicillin, 100 μg ml^{-1} streptomycin, 25 mmol l^{-1} HEPES, 1 mmol l^{-1} sodium pyruvate and 0.1 mmol l^{-1} non-essential amino acids. Regular media were replaced after 16 h by growth media containing 10 mmol l^{-1} sodium butyrate. After incubation for 8 h, the media were changed back to regular growth media. Twenty-four hours later, the virus supernatant was collected, filtered through a 0.45 μm filter and loaded by centrifugation (2,000*g*, 90 min at 32 °C) two times on 50 μg ml^{-1} RetroNectin- (Takara) coated non-tissue six-well plates. Two million to three million cells were transduced per well by centrifugation at 500*g* for 30 min and maintained for 48 h at 37 °C with 5% CO_2 before transferring into culture flasks. Transduced cells with oestrogen receptor fusion proteins were induced with 4-hydroxytamoxifen (500 nM).

***In vivo* model for BCR–ABL1-transformed ALL and bioluminescence imaging.** After cytokine-independent proliferation, BCR–ABL1-transformed ALL cells were labelled with a lentiviral vector encoding firefly luciferase with a neomycin selection marker. After selection with 0.5–2 mg ml^{-1} G418 for 10 days, luciferase-labelled ALL cells were injected into sublethally irradiated (250 cGy) NOD/SCID mice. Human primary leukaemia cells were transduced with a lentiviral firefly luciferase carrying a GFP marker. After expansion of sorted GFP^+ cells, 1×10^5 cells were injected through the tail vein into sublethally irradiated NOD/SCID mice. Bioimaging of leukaemia progression in mice was performed at different time points using an *in vivo* IVIS 100 bioluminescence/optical imaging system (Xenogen). D-Luciferin (Promega) dissolved in PBS was injected intraperitoneally at a dose of 2.5 mg per mouse 15 min before measuring the luminescence signal. General anaesthesia was induced with 5% isoflurane and continued during the procedure with 2% isoflurane introduced through a nose cone. All mouse experiments were subject to institutional approval by the Children's Hospital Los Angeles Institutional Animal Care and Use Committee.

Extraction of bone marrow cells from mice. To avoid inflammation-related effects in $BCL6^{-/-}$ mice[35], bone marrow cells were extracted from young age-matched $BCL6^{+/+}$ and $BCL6^{-/-}$ mice (younger than 6 weeks of age) without signs of inflammation. Bone marrow cells were obtained by flushing cavities of femur and tibia with PBS. After filtration through a 70 μm filter and depletion of erythrocytes using a lysis buffer (BD PharmLyse, BD Biosciences), washed cells were either frozen for storage or subjected to further experiments.

$BCL6^{-/-}$, $Stat5^{fl/fl}$, $Pten^{fl/fl}$ and $p53^{-/-}$ mice. A summary of mouse strains used in this study is provided in Supplementary Table 3. Bone marrow cells from *$BCL6^{-/-}$* (generated in R. Dalla-Favera's laboratory)[36], *$Stat5^{fl/fl}$* (generated in L. Henninghausen's laboratory)[37], *$Pten^{fl/fl}$* (generated in H. Wu's laboratory)[38] and *$p53^{-/-}$* (obtained from Jackson Laboratory) mice were collected and retrovirally transformed by *BCR–ABL1* (ref. 30) in the presence of 10 ng interleukin-7 per milliliter (Peprotech) in RetroNectin- (Takara) coated Petri dishes as described below. All *BCR–ABL1*-transformed ALL cells derived from bone marrow of mice were maintained in Iscove's modified Dulbecco's medium (IMDM, Invitrogen) with GlutaMAX containing 20% fetal bovine serum, 100 IU ml^{-1} penicillin, 100 μg ml^{-1} streptomycin and 50 μM 2-mercaptoethanol. *BCR–ABL1*-transformed ALL cells were propagated only for short periods of time and usually not longer than for 2 months to avoid acquisition of additional genetic lesions during long-term cell culture.

RI-BPI. Homo-dimerization of the amino (N)-terminal Broad Complex, Tramtrack, Bric à brac (BTB) domain of BCL6 forms a lateral groove motif, which is required to recruit co-repressor proteins such as BCL6 co-repressor (BCoR), nuclear receptor co-repressor (N-CoR) and silencing mediator of retinoid and thyroid receptors (SMRT). BCoR, NCoR and SMRT interact in a mutually exclusive manner with an 18-amino-acid motif in the lateral groove of the BCL6 BTB domain to form a BCL6 repression complex[39,40]. A recombinant peptide containing the SMRT BBD (BCL6-binding domain) along with a cell-penetrating TAT domain was able to inhibit the transcriptional repressor activity of BCL6[41]. Based on this initial work, the peptidomimetic molecule RI-BPI with superior potency and stability was developed[25] and used for BCL6-inhibition. RI-BPI represents a retro-inverso TAT-BBD-Fu (fusogenic) peptide[25] that was synthesized by Biosynthesis Inc. (Lewisville, TX) and stored lyophilized at −20 °C until reconstituted with sterile, distilled, degassed water immediately before use. The purity determined by high-performance liquid chromatography–mass spectrometry was 95% or higher. RI-BPI was injected intraperitoneally into mice.

BCR–ABL1 TKI. Imatinib (STI571) and nilotinib (AMN107) were obtained from Novartis Pharmaceuticals or from LC Laboratories. Stock solutions of imatinib were prepared in sterile, distilled water at 10 mmol l^{-1} and stored at −20 °C. Nilotinib was either dissolved in DMSO (dimethyl sulphoxide) or NMP (N-Methyl-2-pyrrolidone) just before administration. Nilotinib dissolved in DMSO was vortexed with four volumes of peanut butter until a homogeneous mixture was formed. Nilotinib (free base) solubilized in NMP was diluted with PEG 300 (polyethylene glycol 300) in a 10/90 (vol/vol) ratio. Cohorts of mice were treated with oral administration of vehicle or nilotinib (25 mg kg^{-1} day^{-1} or 50 mg kg^{-1} day^{-1}) once daily at indicated time points.

Clonality analysis and spectratyping of B-cell populations. Immunoglobulin V_H–DJ_H gene rearrangements were amplified using PCR primers specific for the J558 V_H region gene with a primer specific for the Cμ constant region gene. Using a FAM-conjugated Cμ constant region or a J_H gene-specific primer in a run-off reaction, PCR products were labelled and subsequently analysed on a capillary sequencer (ABI3100, Applied Biosystems) by fragment-length analysis. Sequences of primers used are given in Supplementary Table 4.

Affymetrix GeneChip analysis. Total RNA from cells used for microarray or RT–PCR analysis was isolated by RNeasy (Qiagen) purification. RNA quality was first checked by using an Agilent Bioanalyser (Agilent Technologies). Complementary DNA (cDNA) was generated from 5 μg of total RNA using a poly(dT) oligonucleotide containing a T7 RNA polymerase initiation site and the SuperScript III Reverse Transcriptase (Invitrogen). Biotinylated cRNA was generated and fragmented according to the Affymetrix protocol and hybridized to U133A 2.0 human or 430 mouse microarrays (Affymetrix). After scanning (GeneChip Scanner 3000 7G, Affymetrix) of the GeneChip arrays, the generated CEL files were imported to BRB Array Tool (http://linus.nci.nih.gov/BRB-ArrayTools.html) and processed using the RMA algorithm (Robust Multi-array Average) for normalization and summarization. Relative signal intensities of probe sets were determined by comparing the signal intensity from TKI-treated and untreated cells to the average signal value of the respective cell line or a group of cell lines. The calculated signal ratios of probe sets were visualized as a heatmap with Java Treeview.

Target validation of RI-BPI in human Ph^+ ALL cells. Ph^+ ALL cell lines (BV173, NALM1 and TOM1) were treated with vehicle (control), 10 μmol l^{-1} imatinib or imatinib + 20 μmol l^{-1} RI-BPI for 24 h and maintained in Allprotect (Qiagen) at −80 °C until RNA isolation using an RNeasy Plus kit (Qiagen). RNA integrity was determined using the RNA 6000 Nano LabChip kit on Agilent 2100 Bioanalyser (Agilent Technologies). Two independent samples were analysed for each condition. RNA (1 μg) was hybridized to Agilent 60-mer Whole Human Genome Microarrays (part number G4112A) according to the manufacturer's recommendations. After hybridization, the processed microarrays were scanned with the Agilent DNA microarray scanner (part number G2505C) and extracted with Agilent Feature Extraction software version 8.5 (GE1-v5_10_Apr08). For computational analysis of signal, we used the dye-normalized signal after surrogate algorithm (gProcessedSignal) extracted from the .txt files and process for each array and for all the probes. This value was subjected to $\log_2$ transformation and median array normalization. The fold changes of imatinib compared with control and (imatinib + RI-BPI) compared with imatinib were calculated for each cell line and for each gene. A data set containing previously identified BCL6 target genes (obtained from Nimblegen arrays) was mapped into the Agilent probe sets using the Agilent and NimbleGen array annotation files. To determine if two data sets differed significantly, we compared the fold change in BCL6 target genes with the fold change in BCL6 non-target genes for each data set (imatinib compared with control, and imatinib + RI-BPI compared with imatinib) by the Kolmogorov–Smirnov test[42]. The Kolmogorov–Smirnov test deter-

mines if two data sets (gene expression values for BCL6 target genes and non-target genes) differ significantly. Heat maps and other analysis were obtained using the R statistical software (http://www.r-project.org).

ChIP-on-chip analysis. ChIPs were performed with modifications as described[43]. Briefly, 2.5×10^7 Ph^+ ALL cell lines (BV173, NALM1 and TOM1) were treated with or without 10 μmol l^{-1} imatinib for 24 h. Then the cells were double cross-linked with 2 mmol l^{-1} EGS cross linker and 1% formaldehyde. After sonication, immunoprecipitations were performed using 5 μg BCL6 (N3, Santa Cruz Biotechnology) or control IgG antibody (Sigma-Aldrich) from the chromatin fragments of 2.5×10^7 human Ph^+ ALL cells. After validation of enrichment by Q-ChIP, BCL6 or control IgG, ChIP products and their respective input genomic fragments were amplified by ligation-mediated PCR. The products were co-hybridized with the respective input samples to NimbleGen promoter arrays (human genome version 35). Quantitative ChIP was performed again at this stage for selected positive control loci to verify that the enrichment ratios were retained. The genomic products of two biological ChIP replicates were labelled with Cy5 (for ChIP products) and Cy3 (for input) and co-hybridized on custom-designed genomic tiling arrays generated by NimbleGen Systems. These high-density tiling arrays contained 50-residue oligonucleotides with an average overlap of 25 bases, omitting repetitive elements. After hybridization, the relative enrichment for each probe was calculated as the signal ratio of ChIP to input. Peaks of enrichment for BCL6 relative to input were captured with a five-probe sliding window, and the results were uploaded as custom tracks into the University of California Santa Cruz genome browser and graphically represented as histograms. Two replicates were performed with each condition.

Data analysis of ChIP-on-chip experiments. To identify target genes of BCL6 in these experiments, we computed the log-ratio between the probe intensities of the ChIP product and input and took moving averages of log-ratio of three neighbouring probes and determined the maximum value for each gene promoter and the random permutation probes as background control[44]. The cut-off for each array was established as higher than the 99th percentile of the 24,175 log-ratio values generated from random permutation probes. A locus with maximum moving average above cut-offs in two replicates was considered a potential binding site. Because this high stringent-overlapping approach can produce a high false-negative rate, we also computed the correlations among peaks between the replicates to rescue promoters that did not pass cut-off in one replicate. We calculated the Pearson correlation coefficient of the probe's signal of the promoter between replicates, and promoters with a correlation higher that 0.8 were rescued and included in our final set of BCL6 targets. In addition, all peaks were mapped back to the genome using BLAT (the BLAST-like Alignment Tool, http://genome.ucsc.edu) to identify genes on opposite strands that could be regulated from the same bidirectional promoter. Two genes were considered to be bidirectional partners when they were located on the opposite strands in a 'head-to-head' orientation and their transcription start sites were separated by less than 0.5 kilobases.

Comparative genomic hybridization. To analyse genetic instability and acquisition of genetic lesions during long-term cell culture, genomic DNA of BCR–ABL1-transformed $BCL6^{+/+}$ and $BCL6^{-/-}$ ALL cells was extracted after culturing for 4 months. Genomic DNA was isolated using the PureLink genomic DNA kit (Invitrogen). Three samples of each ALL type were co-hybridized with genomic DNA extracted from normal untransformed mouse cells to NimbleGen mouse 720k Whole-Genome Tiling arrays (NimbleGen Systems) in accordance with the manufacturer's recommendations. Copy number variations were analysed using the FASST-segmentation algorithm in Nexus software (BioDiscovery). Copy-number analysis was performed using a significance threshold of 1×10^{-7} and a $\log_2$ ratio cut-off at ± 0.2 for regions sized 1,000 kilobase pairs.

Senescence-associated β-galactosidase assay. Senescence-associated β-galactosidase activity was performed on cytospin preparations as described[21]. Briefly, a fixative solution (0.25% glutaraldehyde, 2% paraformaldehyde in PBS pH 5.5 for mouse cells and pH 6 for human cells) was freshly generated. To this end, 1 g paraformaldehyde was dissolved in 50 ml PBS at pH 5.5 by heating followed by addition of 250 μl of a 50% stock glutaraldehyde solution. 1× X-gal staining solution was prepared as follows (10 ml): 9.3 ml PBS/$MgCl_2$, 0.5 ml 20× KC solution (that is, 820 mg $K_3Fe(CN)_6$ and 1,050 mg $K_4Fe(CN)_6 \times 3H_2O$ in 25 ml PBS) and 0.25 ml 40× X-gal (that is, 40 mg 5-bromo-4-chloro-3-indolyl β-D-galactoside per milliliter of *N,N*-dimethylformamide) solution were mixed. For *BCR–ABL1*-transformed ALL cells, 100,000 cells per cytospin were used (700 r.p.m., 8 min). The fixative solution was pipetted on the cytospins and incubated for 10 min at room temperature, then washed twice for 5 min in PBS/$MgCl_2$. Cytospin preparations were submerged in 1× X-gal solution, incubated overnight at 37 °C in a humidified chamber and washed twice in PBS. Slides were mounted before they dried.

Western blotting. Cells were lysed in CelLytic buffer (Sigma) supplemented with 1% protease inhibitor cocktail (Pierce). Ten micrograms of protein mixture per sample were separated on NuPAGE (Invitrogen) 4–12% Bis-Tris gradient gels and transferred on PVDF membranes (Immobilion, Millipore). To detect mouse and human proteins by western blot, primary antibodies were used with the WesternBreeze immunodetection system (Invitrogen). The following antibodies were used: human BCL6 (clones D8 and N3, Santa Cruz Biotechnology), mouse BCL6 (rabbit polyclonal, Cell Signaling Technology), Arf (4C6/4, Cell Signaling Technology), p53 (1C12, Cell Signaling Technology), PTEN (A2B1, Santa Cruz), global Stat5 (3H7, Cell Signaling Technology) and phospho-Y694 Stat5 (14H2, Cell Signaling Technology). Antibodies against β-actin were used as a loading control (C4, Santa Cruz).

Flow cytometry. Antibodies against mouse CD19 (1D3), B220 (RA3-6B2), CD3 (17A2), CD43 (S7), CD45.1 (A20), CD45.2 (104), CD44 (IM7 and G44-26) and c-Kit (2B8) as well as respective isotype controls were purchased from BD Biosciences. For apoptosis analyses, Annexin V, propidium iodide and 7-AAD were used (BD Biosciences).

Cell viability assay. Fifty thousand *BCR–ABL1*-transformed ALL cells per well were seeded in a volume of 100 μl B-cell medium on Optilux 96-well plate (BD Biosciences). Imatinib was diluted in medium and added at the indicated concentration in a total culture volume of 150 μl. After culturing for 3 days, 15 μl of Resazurin (R&D) was added on each well and incubated for 4 h at 37 °C. The fluorescence was read at 535 nm and the reference wavelength was 590 nm. Fold changes were calculated using baseline values of untreated cells as a reference (set to 100%).

Colony-forming assay. The methylcellulose colony-forming assays were performed with 10,000 *BCR–ABL1*-transformed mouse $BCL6^{-/-}$ or $BCL6^{+/+}$ or 10,000 human *BCR–ABL1* ALL cells. Cells were re-suspended in MethoCult medium (StemCell Technologies) and cultured on dishes (3 cm diameter) with an extra water supply dish to prevent evaporation. After 7–14 days, colonies were counted.

Cell-cycle analysis. For cell-cycle analysis in *BCR–ABL1* ALL cells, the BrdU flow cytometry kit for cell-cycle analysis (BD Biosciences) was used according to manufacturer's instructions. BrdU incorporation (APC-labelled anti-BrdU antibodies) was measured with DNA content (7-amino-actinomycin-D) in fixed and permeabilized cells. The analysis was gated on viable cells that were identified based on scatter morphology[45].

***In vivo* toxicology studies of RI-BPI/nilotinib combinations.** Fifteen adult male C57BL/6 mice were purchased from the National Cancer Institute and randomized in three groups of five. One group was exposed to intraperitoneal administration of RI-BPI 20 mg kg^{-1} of body weight three times a week; the second group was treated with RI-BPI 20 mg kg^{-1} of body weight three times a week plus nilotinib 25 mg kg^{-1} of body weight three times a week by oral gavage. A third group of five mice was treated with vehicle and used as controls. The mice were observed, examined and weighed every other day during the treatment period. Blood was collected at the end of the treatment by retro-orbital bleeding under anaesthesia. All mice were euthanized by CO_2 aspiration and the organs were harvested, weighed and macroscopically examined. Histology sections were prepared with haematoxylin and eosin staining. Pictures were taken using a digital camera (Olympus DP72) attached to a light microscope (Axioskop, Carl Zeiss) with ×4 and ×20 Plan Neofluar objectives (Carl Zeiss).

30. Pear, W. S. *et al.* Efficient and rapid induction of a chronic myelogenous leukemia-like myeloproliferative disease in mice receiving P210 bcr/abl-transduced bone marrow. *Blood* **92,** 3780–3792 (1998).
31. Onishi, M. *et al.* Identification and characterization of a constitutively active STAT5 mutant that promotes cell proliferation. *Mol. Cell. Biol.* **18,** 3871–3879 (1998).
32. Godar, S. *et al.* Growth-inhibitory and tumor- suppressive functions of p53 depend on its repression of CD44 expression. *Cell* **134,** 62–73 (2008).
33. Kumar, M. S. *et al.* Dicer1 functions as a haploinsufficient tumor suppressor. *Genes Dev.* **23,** 2700–2704 (2009).
34. Soneoka, Y. *et al.* A transient three-plasmid expression system for the production of high titer retroviral vectors. *Nucleic Acids Res.* **23,** 628–633 (1995).
35. Dent, A. L., Shaffer, A. L., Yu, X., Allman, D. & Staudt, L. M. Control of inflammation, cytokine expression, and germinal center formation by BCL-6. *Science* **276,** 589–592 (1997).
36. Ye, B. H. *et al.* The BCL-6 proto-oncogene controls germinal-centre formation and Th2-type inflammation. *Nature Genet.* **16,** 161–170 (1997).
37. Cui, Y. *et al.* Inactivation of Stat5 in mouse mammary epithelium during pregnancy reveals distinct functions in cell proliferation, survival, and differentiation. *Mol. Cell. Biol.* **24,** 8037–8047 (2004).
38. Groszer, M. *et al.* Negative regulation of neural stem/progenitor cell proliferation by the Pten tumor suppressor gene in vivo. *Science* **294,** 2186–2189 (2001).
39. Ahmad, K. F. *et al.* Mechanism of SMRT corepressor recruitment by the BCL6 BTB domain. *Mol. Cell* **12,** 1551–1564 (2003).
40. Ghetu, A. F. *et al.* Structure of a BCOR corepressor peptide in complex with the BCL6 BTB domain dimer. *Mol. Cell* **29,** 384–391 (2008).
41. Polo, J. M. *et al.* Specific peptide interference reveals BCL6 transcriptional and oncogenic mechanisms in B-cell lymphoma cells. *Nature Med.* **10,** 1329–1335 (2004).
42. Chakravarti, L&. Roy, (1967). Handbook of Methods of Applied Statistics, Volume I, John Wiley and Sons, pp. 392-394. (1967).
43. Ci, W. *et al.* The BCL6 transcriptional program features repression of multiple oncogenes in primary B cells and is deregulated in DLBCL. *Blood* **113,** 5536–5548 (2009).

44. Polo, J. M. *et al.* Transcriptional signature with differential expression of BCL6 target genes accurately identifies BCL6-dependent diffuse large B cell lymphomas. *Proc. Natl Acad. Sci. USA* **104,** 3207–3212 (2007).

45. Trageser, D. *et al.* Pre-B cell receptor-mediated cell cycle arrest in Philadelphia chromosome-positive acute lymphoblastic leukemia requires IKAROS function. *J. Exp. Med.* **206,** 1739–1753 (2009).

doi:10.1038/nature09883

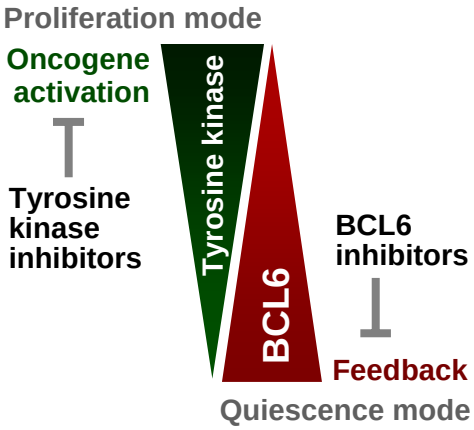

Supplementary Figure 1: *Scenario - Dual targeting of oncogenic tyrosine kinase signaling and BCL6-dependent feedback in Ph⁺ B cell lineage ALL*

Proposed concept of dual targeting of oncogenic tyrosine kinase signaling (e.g. BCR-ABL1, FLT3, JAK2, PDGFR) and BCL6-dependent feedback signaling in tyrosine kinase-driven leukemia. Current approaches for targeted therapy of acute lymphoblastic leukemia mainly focus on the development of more potent tyrosine kinase inhibitors (TKI) that also cover mutant tyrosine kinases. While effective TKI induce cell death in the bulk of the rapidly dividing tyrosine kinase-dependent leukemia population ("**proliferation mode**"), TKI typically fail to eradicate quiescent leukemia-initiating cells ("**quiescence mode**").

BCL6 provides protection in response to TKI-treatment of leukemia cells by suppression of ARF/p53-dependent apoptosis and by preventing cellular senescence. In this situation, the cells are highly drug-resistant and in "quiescence mode". In fact, BCL6 itself induces cellular quiescence by transcriptional repression of Myc (reference 14). Upon cessation of TKI-treatment, oncogenic tyrosine kinase activity resumes and the leukemia cells revert into "proliferation mode", which represents the onset of leukemia recurrence after initially successful treatment. Currently, a peptide inhibitor (RI-BPI; reference 25) and a small molecule inhibitor (79-6; reference 29) are available to block the ability of BCL6 to recruit its co-repressors (NCoR, SMRT, BCoR). We propose that dual targeting of tyrosine kinase signaling (TKI, "proliferation mode") and BCL6-dependent protective feedback (BCL6 inhibitors, "quiescence mode") represents a novel strategy to eradicate drug-resistant and leukemia-initiating subclones in tyrosine kinase-driven leukemia.

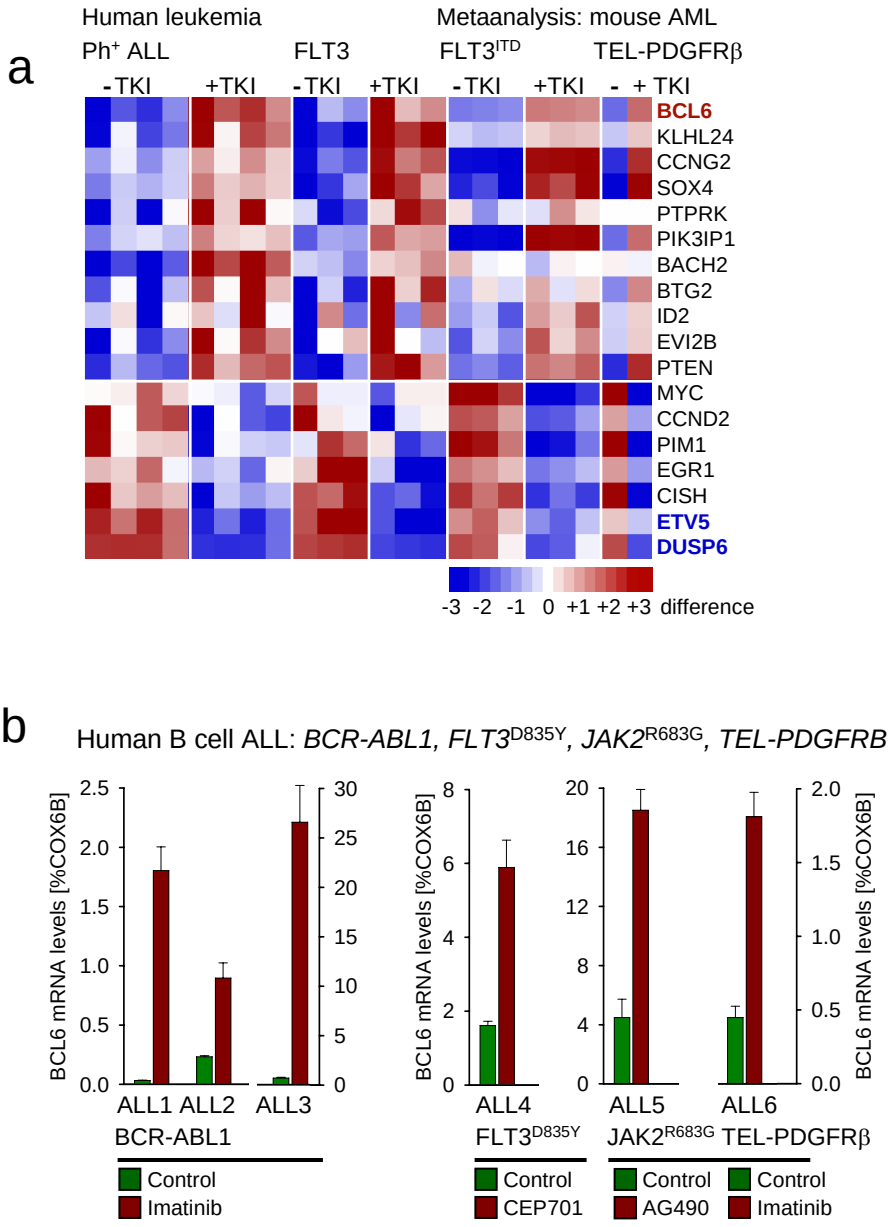

Supplementary Figure 2: *Tyrosine kinase-driven leukemia cells respond to oncogene withdrawal by upregulation of BCL6*

(a) Seven human leukemia cell lines carrying the BCR-ABL1 kinase (4 Ph^+ ALL, 3 CML) were treated with or without Imatinib (10 µmol/l) for 16 hours. In addition, a meta-analysis of gene expression data of mouse myeloid leukemia cells carrying $FLT3^{ITD}$ and TEL-PDGFRβ kinases that were treated with MLN518 (0.5 µmol/l, 4 hours) or Imatinib (5 µmol/l, 4 hours) is shown. Gene expression data were sorted based on ratio [$\log_2$] of gene expression values in treated vs untreated leukemia cells. Microarray data used in this analysis are available from GEO under accession numbers GSE23743, GSE11794 and GSE24493. (b) TKI-induced upregulation of BCL6 was confirmed by quantitative RT-PCR in six cases of tyrosine kinase-driven leukemia (3 Ph^+ ALL, 1 *FLT3*^{D835Y} ALL, 1 *JAK2*^{R683G} ALL, 1 *TEL-PDGFR*β ALL; means of triplicate measurements ± SD).

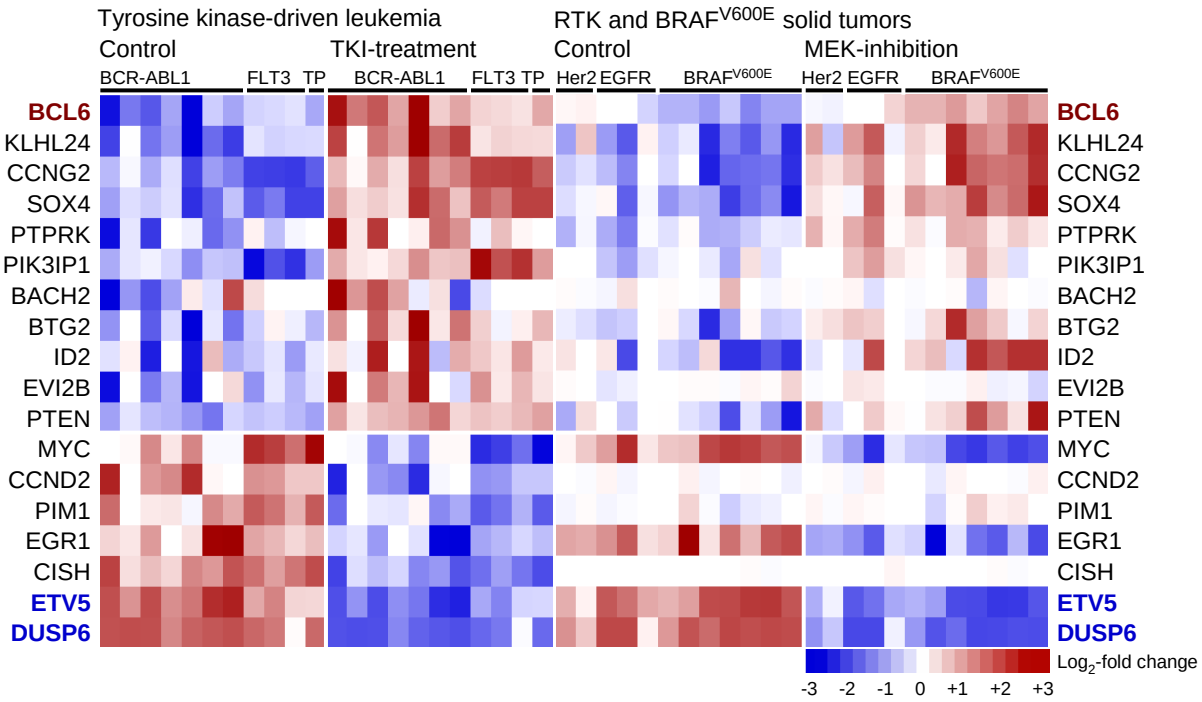

Supplementary Figure 3: *Similarities between TKI-induced gene expression changes in leukemia cells and MEK inhibition in BRAF^{V600E} mutant solid tumors*

As set of genes with a similar pattern of regulation by TKI across multiple oncogenic tyrosine kinases was identified (see Supplemental Figure 2a). Gene expression values in BCR-ABL1 (7 Ph$^+$ ALL), FLT3^{ITD} AML (FLT3; n=3) and TEL-PDGFRβ AML (TP; n=1) before and after TKI-treatment were plotted against gene expression values in solid tumor cells expressing oncogenic receptor-type tyrosine kinases (RTK) or mutant BRAF^{V600E} (reference 10; GEO accession number GSE10086). Oncogenic RTK include Her2-overexpressing breast cancer (n=2; BT474, SKBR3), EGFR-mutant bronchioalveolar adenocarcinoma (n=1; H1650) and EGFR-overexpressing epidermoid and breast cancer (n=2; A431, MDA468) cell lines. EGFR-mutant and –overexpressing cell lines are collectively denoted as "EGFR".

Human leukemia cell lines carrying the BCR-ABL1 kinase were treated with Imatinib (10 µmol/l) for 16 hours. Mouse myeloid leukemia cells carrying FLT3^{ITD} and TEL-PDGFRβ kinases were treated with MLN518 (0.5 µmol/l, 4 hours) or Imatinib (5 µmol/l, 4 hours). MEK-inhibition was performed with 50 nmol/l PD0325901 for 8 hours.

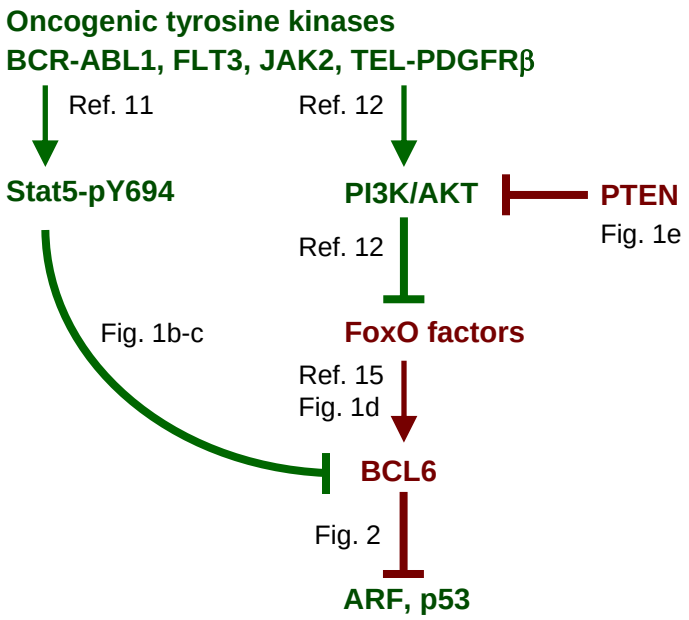

Supplementary Figure 4: *Regulation of BCL6 expression in tyrosine kinase-driven leukemias*

Oncogenic tyrosine kinases negatively regulate BCL6 expression via Stat5 (direct repression of BCL6 transcription (ref. 13 and Fig. 1b-c) and PI3K/AKT (inactivation of FoxO factors; ref. 12). PTEN antagonizes PI3K/AKT function and thereby favors activation of FoxO factors and hence, transcriptional activation of BCL6. Here we show that PTEN is required for transcriptional activation of BCL6 (Fig. 1e) and, hence, BCL6-mediated repression of ARF and p53 (Fig. 2).

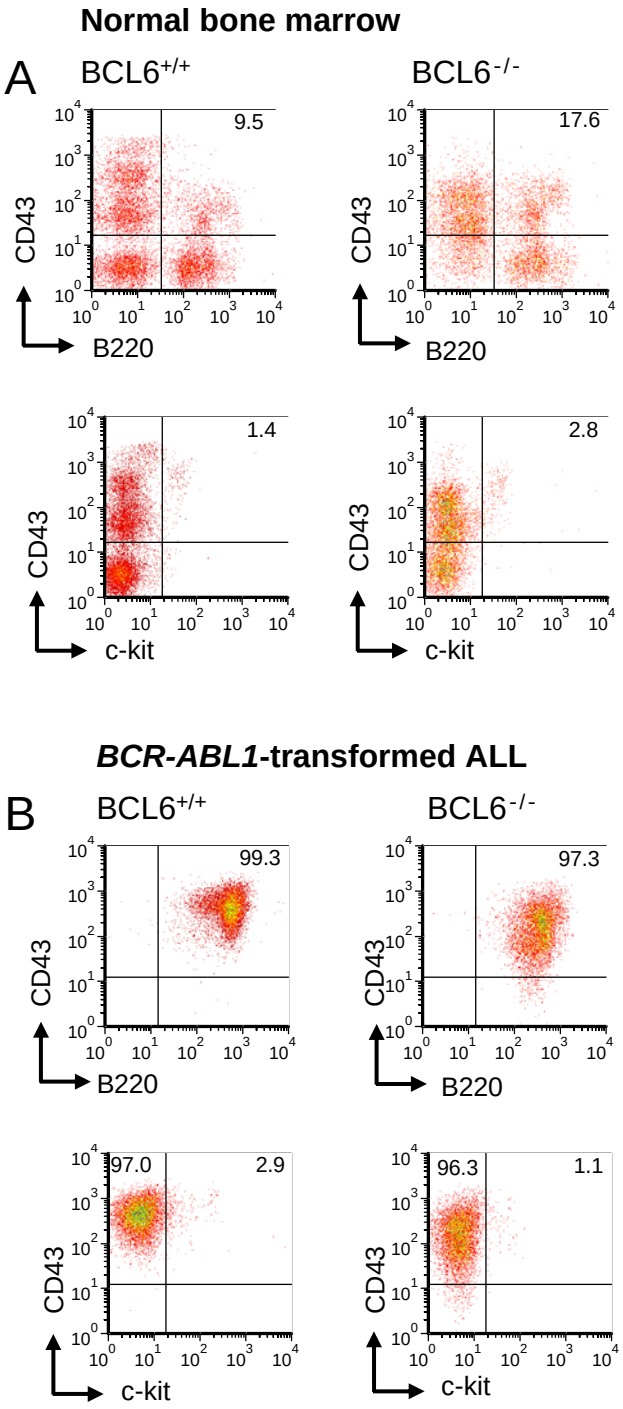

Supplementary Figure 5: *BCR-ABL1 transforms comparable B cell precursor subsets in BCL6$^{+/+}$ and BCL6$^{-/-}$ mice*

Rationale: This experiment addresses the question of whether the same cell type is transformed by *BCR-ABL1* in BCL6$^{+/+}$ and BCL6$^{-/-}$ bone marrow. While late pre-BII cells are diminished in BCL6$^{-/-}$ mice[14], the pro- and pre-BI subsets, which represent the target of *BCR-ABL1*-mediated transformation, are slightly expanded in the bone marrow of BCL6$^{-/-}$ mice (A).

The CD43^{+} B220^{+} c-Kit$^{low/-}$ pro-/pre-BI cell population represents the target of *BCR-ABL1*-mediated transformation and is present both in BCL6$^{+/+}$ and BCL6$^{-/-}$ bone marrow (A). *BCR-ABL1*-transformed ALL cells from BCL6$^{+/+}$ and BCL6$^{-/-}$ bone marrow have a similar pro-/pre-BI cell phenotype and express high levels of CD43 and B220 and low levels of the pro-B cell antigen c-Kit (B). As determined by immunoglobulin heavy chain spectratyping, both BCL6$^{+/+}$ and BCL6$^{-/-}$ BCR-ABL1 ALL cells carry a clonal V_H-DJ_H rearrangement. Splenic B cells were used as positive control to depict a polyclonal repertoire of V_H-DJ_H junctions (C).

Note: Besides *BCR-ABL1*, also retroviral overexpression of the Myc proto-oncogene leads to transformation of BCL6$^{-/-}$ progenitor cells and growth-factor-independent leukemia (C.D., unpublished observation).

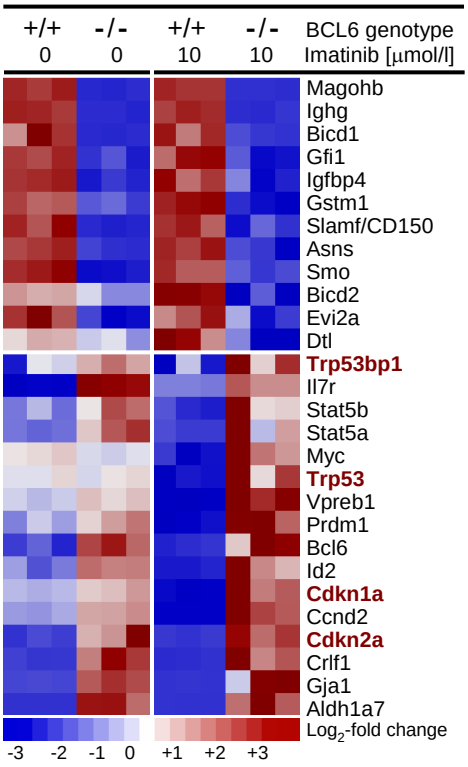

Supplementary Figure 6: *BCL6-dependent gene expression changes in BCR-ABL1 ALL cells*

Gene expression changes in response to Imatinib-treatment were studied in BCL6$^{-/-}$ and BCL6$^{+/+}$ *BCR-ABL1* ALL cells by Affymetrix GeneChip analysis and data were sorted based on the ratio of gene expression values in BCL6$^{-/-}$ and BCL6$^{+/+}$ *BCR-ABL1* ALL cells in the presence of Imatinib. Microarray data used in this analysis are available from GEO under accession number GSE20987.

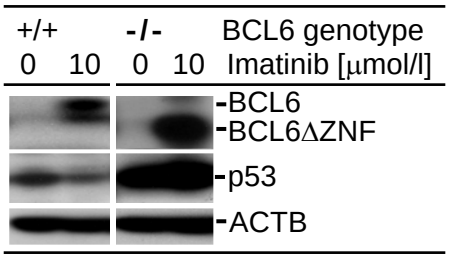

Supplementary Figure 7: *TKI-treatment results in BCL6-mediated downregulation of p53*

Previous studies showed that treatment of BCR-ABL1 leukemia cells with Imatinib paradoxically results in inhibition of p53 accumulation in response to DNA damage. Likewise, treatment of BCR-ABL1 ALL cells with 10 μmol/l Imatinib resulted in downregulation of p53 in parallel with BCL6 upregulation (left panel). In $BCL6^{-/-}$ BCR-ABL1 ALL, p53 levels are constitutively high and further increased by Imatinib-treatment (right panel). Hence, BCL6 is required for Imatinib-induced downregulation of p53 in Ph^{+} ALL.

For Western blotting, antibodies against BCL6 and p53 were used and β-actin as loading control. BCL6ΔZNF denotes a truncated protein that is still expressed in "$BCL6^{-/-}$" mice, in which critical zinc finger domains of BCL6 are deleted (reference 36).

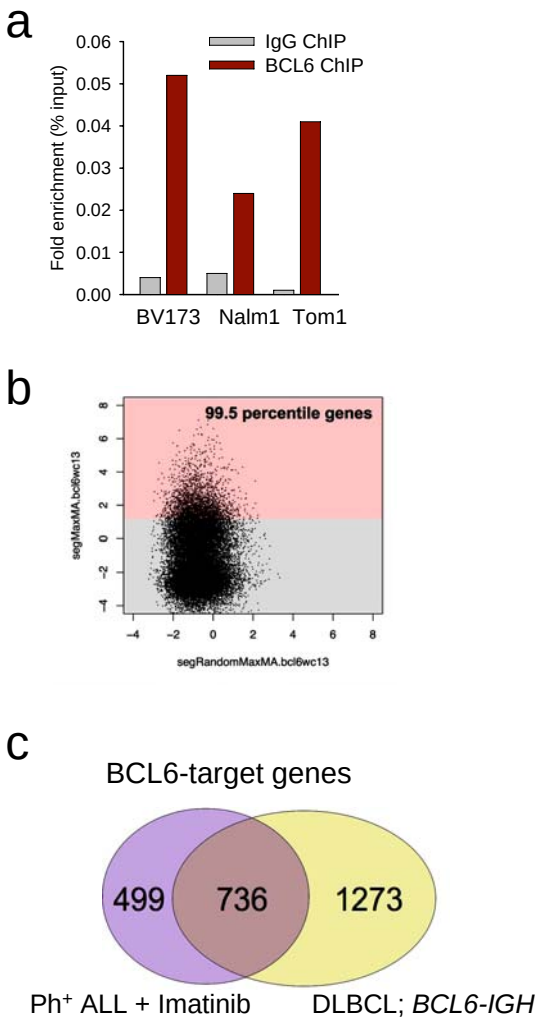

Supplementary Figure 8: *BCL6 ChIP-on-chip analysis of Ph⁺ ALL cell lines*

(a) ChIP was performed with BCL6 antibodies followed by QPCR to detect the BCL6 binding site in exon 1 of the *BCL6* locus in Tom1, Nalm1 and BV173 ALL cell lines treated with Imatinib. Treatment with Imatinib induces BCL6 expression. Red bars denote BCL6-ChIP and gray bars denote control IgG.

(b) A random permutation analysis was performed using a sliding window of three oligos to identify BCL6 binding peaks in the Ph⁺ ALL cell lines (the panel shows one of the Nalm1 replicates as an example). The graph shows the non-zero centered comparison between BCL6 peaks (y-axis) vs. a random permutation of the oligos (x-axis). The red field at the top denotes those peaks scoring > than 99.5 percentile, which captured ~1,300 genes as being true positive BCL6 targets in Nalm1 cells. Single locus validation confirmed > 95% accuracy.

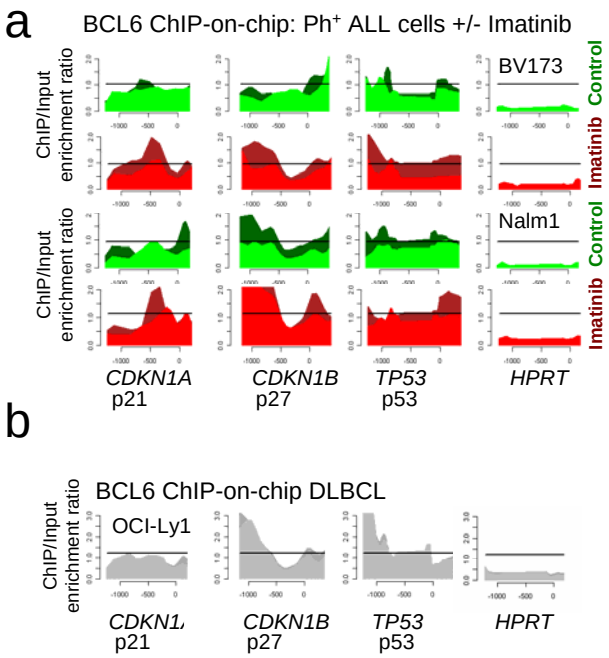

Supplementary Figure 9: *Specific recruitment of BCL6 to CDKN1A, CDKN1B and TP53 promoters in Ph+ ALL cells*

Three Ph+ ALL cell lines (BV173, Nalm1, Tom1) were treated in the presence or absence of Imatinib (10 μmol/l) and subjected to BCL6 ChIP-on-chip analysis. BV173 and Nalm1 are shown here, ChIP profiles for Tom1 are shown in Fig. 2. The y-axis indicates enrichment versus input and the x-axis the location of probes within the respective loci relative to the transcriptional start site. The dark and light green (Control) or red (Imatinib) tracings depict two replicates. Recruitment to *CDKN1A*, *CDKN1B*, *TP53* and *HPRT* (negative control) is shown in Ph+ ALL cell lines BV173 and Nalm1 and one DLBCL cell line (OCI-Ly1).

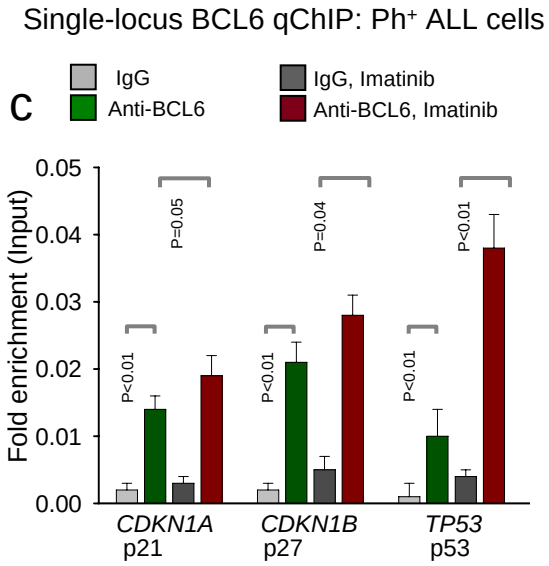

Supplementary Figure 10: *Single-locus quantitative ChIP verification of BCL6 recruitment to CDKN1A, CDKN1B and p53 promoters.*

Single locus quantitative ChIP shows recruitment of BCL6 to *CDKN1A* (p21), *CDKN1B* (p27) and *TP53* promoters. Means of fold-enrichment (duplicate measurements for three cell lines, n=3; means ± SD) are indicated. The cell lines used are BV173, Nalm1 and TOM1.

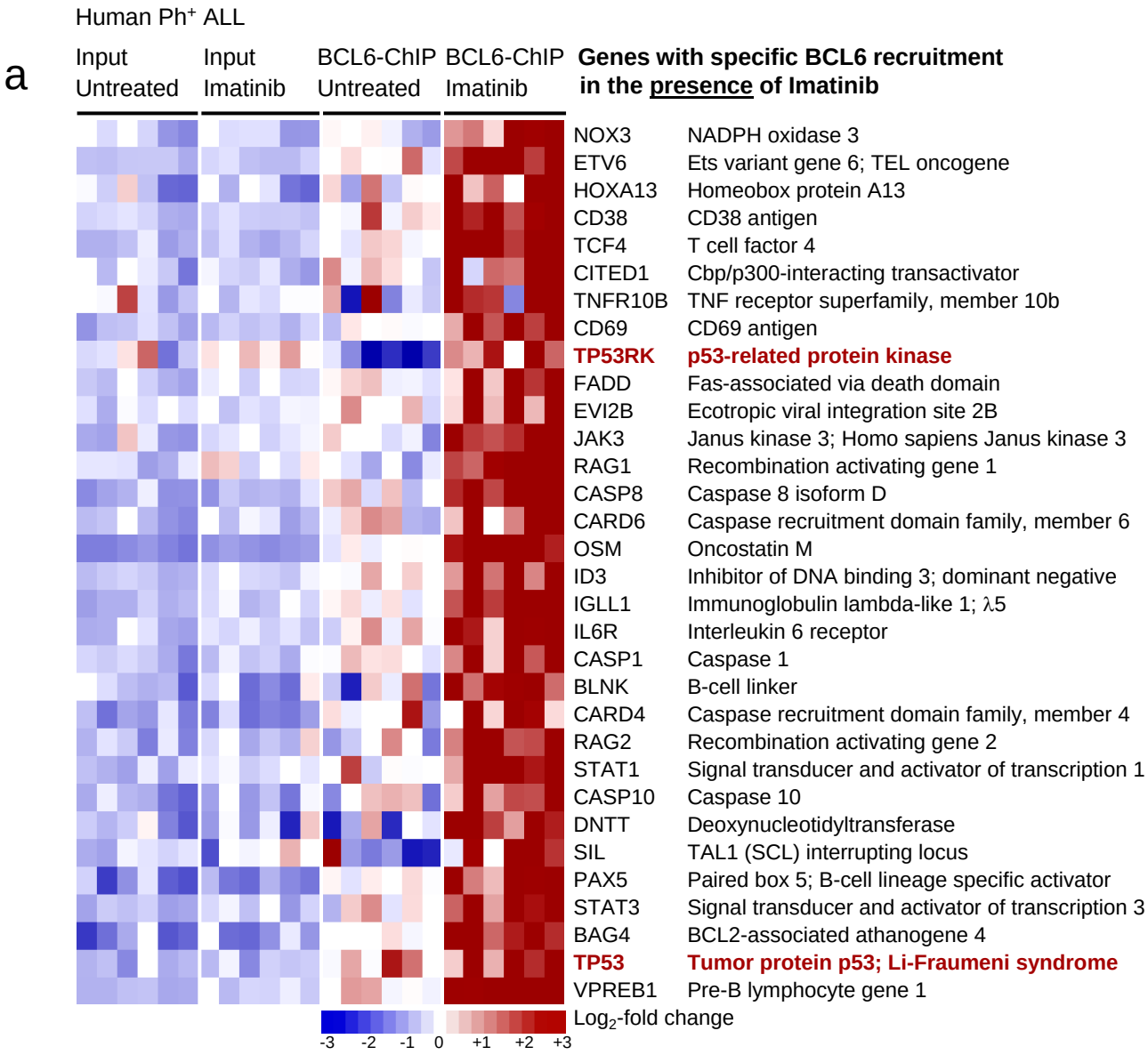

Supplementary Figure 11: *BCL6 target genes with specific recruitment of BCL6 in Imatinib-treated Ph+ ALL cells*

Three Ph+ ALL cell lines (BV173, Nalm1, Tom1) were treated in the presence or absence of Imatinib (10 μmol/l) and subjected to BCL6 ChIP-on-chip analysis. Most of the BCL6 target genes show BCL6 recruitment only in the presence of Imatinib-treatment. The heatmap presented in (a) depicts a list of genes that are specifically targeted by BCL6 in the presence of Imatinib (1,024 target genes). For instance, *TP53* only shows significant enrichment of BCL6 to its promoter when Ph+ ALL were treated with Imatinib (highlighted in red). The heatmap presented in (b) shows gene loci with significant recruitment of BCL6 also when Ph+ ALL were not treated with Imatinib. For instance, the *CDKN1B* (p27) and *GADD45B* loci show significant binding of BCL6 even in the absence of Imatinib-treatment (highlighted in red). 211 genes are in this group. Table (c) summarizes how Imatinib-treatment impacts on BCL6-recruitment in Ph+ ALL cells. Only 5 loci show specific recruitment of BCL6 in the absence of Imatinib. Recruitment of BCL6 to these loci, however, needs independent verification by single locus quantitative ChIP as we performed here for *CDKN1A* (p21), *CDKN1B* (p27), *GADD45B* and *TP53*. ChIP-on-chip data are available from GEO under accession number GSE24426.

b

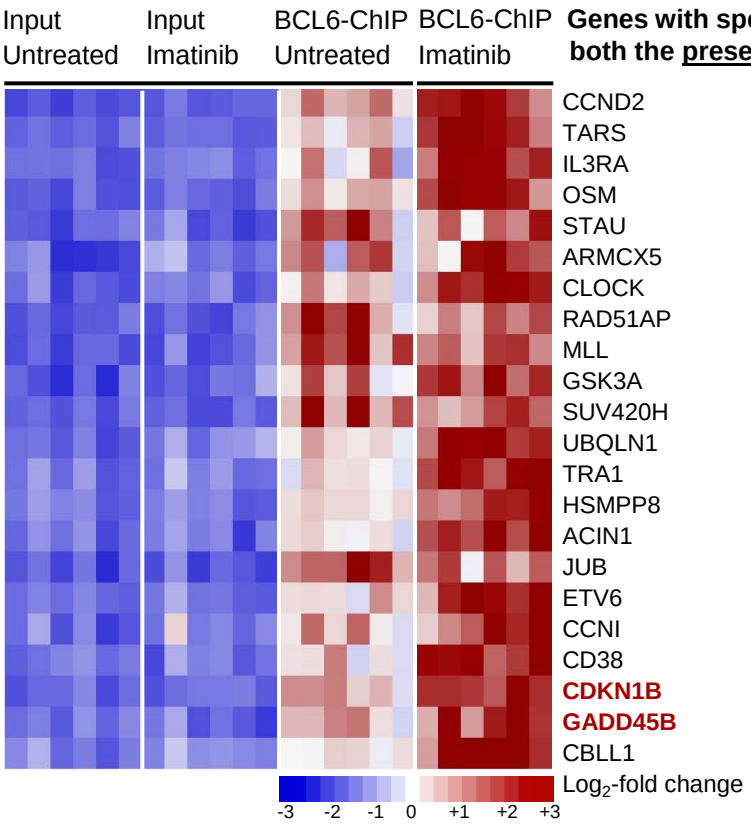

c

BCL6 recruitment	
1,235	In the presence of Imatinib
1,024	Only in the presence of Imatinib
211	Also in the absence of Imatinib
5	Only in the absence of Imatinib
1,240	Total BCL6 target genes in Ph^+ ALL

Supplementary Figure 11 (continued): *BCL6 target genes with specific recruitment of BCL6 in Imatinib-treated Ph^+ ALL cells*

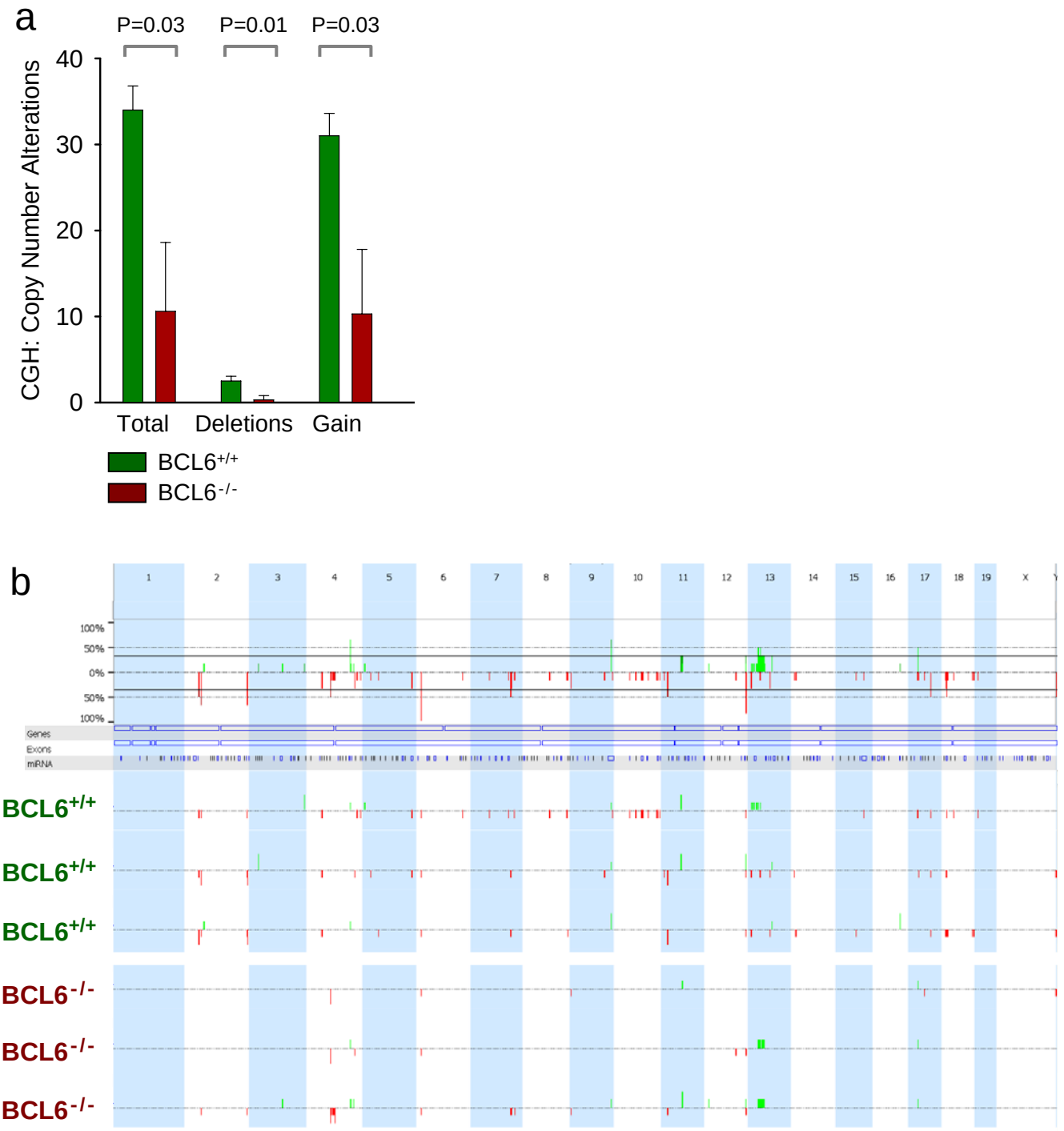

Supplementary Figure 12: *Analysis of genetic instability in BCL6$^{+/+}$ and BCL6$^{-/-}$ BCR-ABL1-transformed ALL cells*

Comparative genomic hybridization (CGH) analysis (NimbleGen, 720k Whole Genome Tiling arrays) of three transformed BCL6$^{+/+}$ and BCL6$^{-/-}$ BCR-ABL1 leukemias was performed. **a.** The frequencies of copy number alterations in BCR-ABL1-transformed BCL6$^{+/+}$ and BCL6$^{-/-}$ leukemias were determined (mean values ± SD; n=3) and depicted for all events, deletions and gains/amplifications. In **b**., genetic lesions that were specifically acquired either in BCL6$^{+/+}$ or BCL6$^{-/-}$ leukemia cells are depicted. In **c**. a distribution of all copy number alterations over the mouse chromosomes is depicted. CGH array data are available from GEO under accession number GSE24400.

c

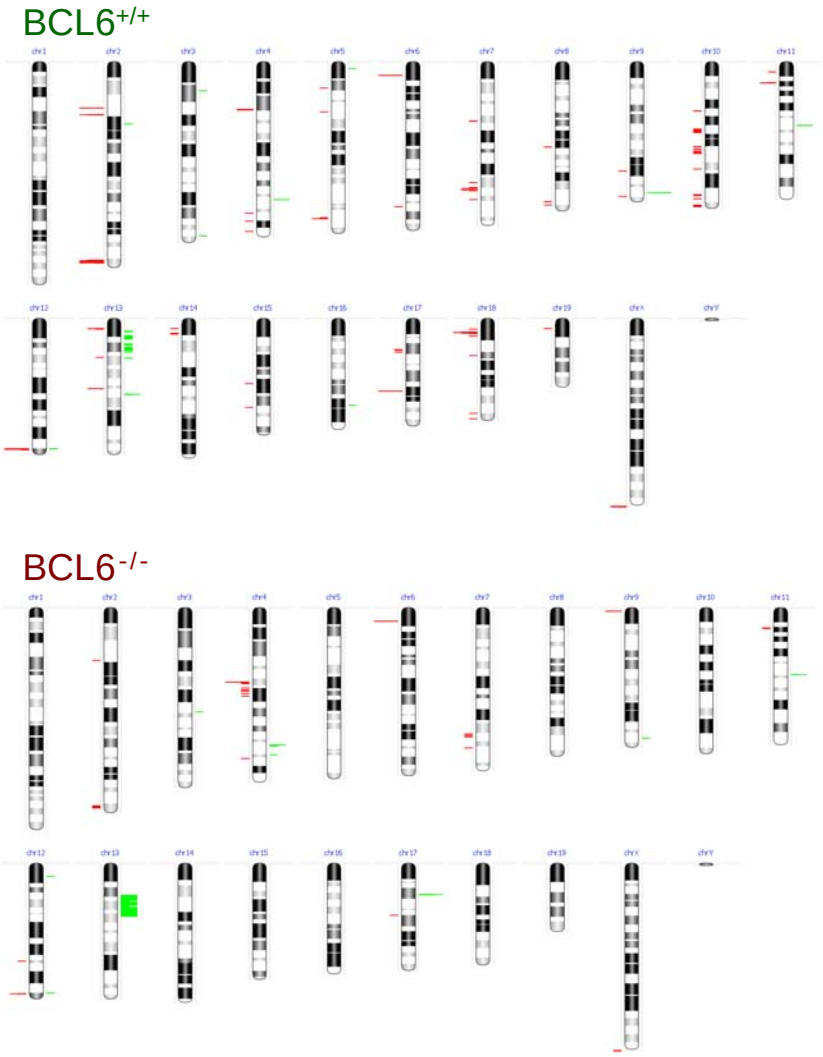

Supplementary Figure 12 continued

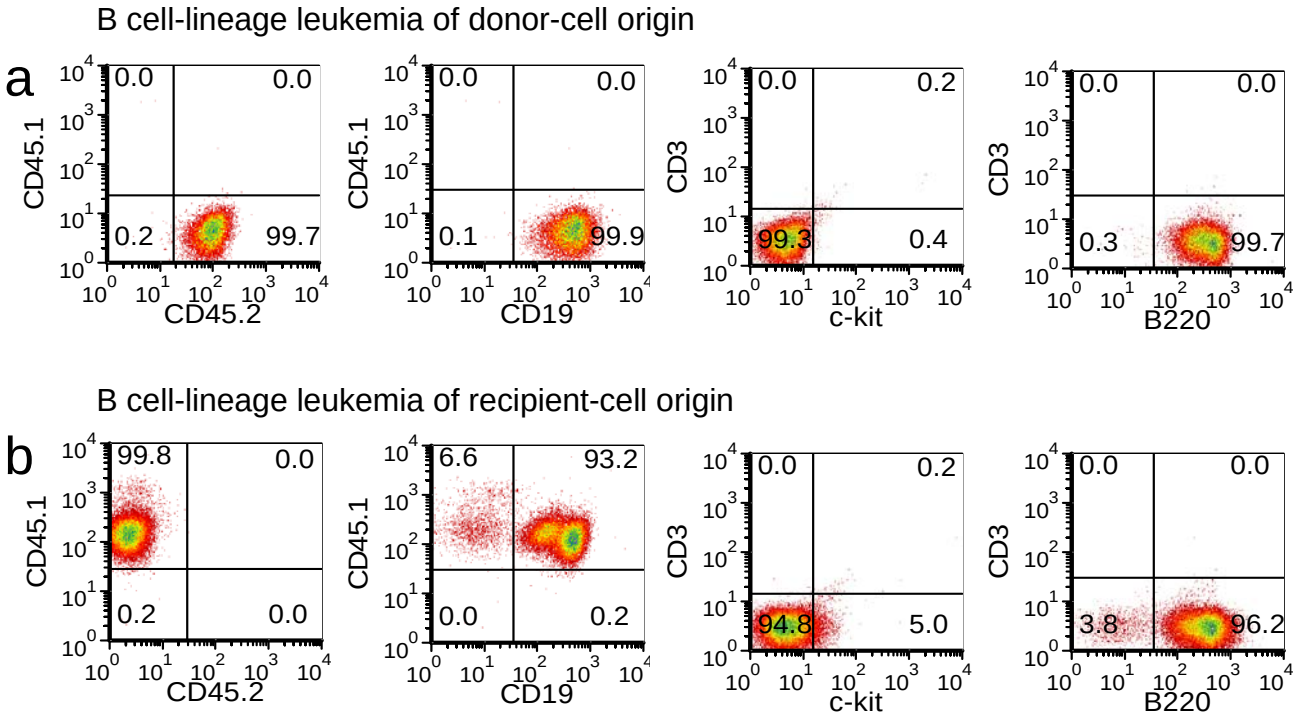

Supplementary Figure 13: *Phenotypic analysis of donor- or recipient-origin of leukemia developing in irradiated NOD/SCID mice*

BCR-ABL1-transduced ALL cells from BCL6$^{+/+}$ or BCL6$^{-/-}$ mice express CD45.2 but not CD45.1. These leukemia cells can be identified as CD45.2^{+} cells after injection into CD45.1^{+} NOD/SCID recipient mice (**a**). In some cases, irradiated NOD/SCID recipient mice develop endogenous leukemia, in particular in older mice (see asterisks in Figure 3b, where mice were monitored for 250 days). Endogenous leukemia cells can be identified as CD45.1^{+} cells of recipient origin (**b**). For further characterization, leukemia cells were stained for expression of the B cell antigens CD19 and B220, the T cell antigen CD3 and c-kit to identify particularly immature cells.

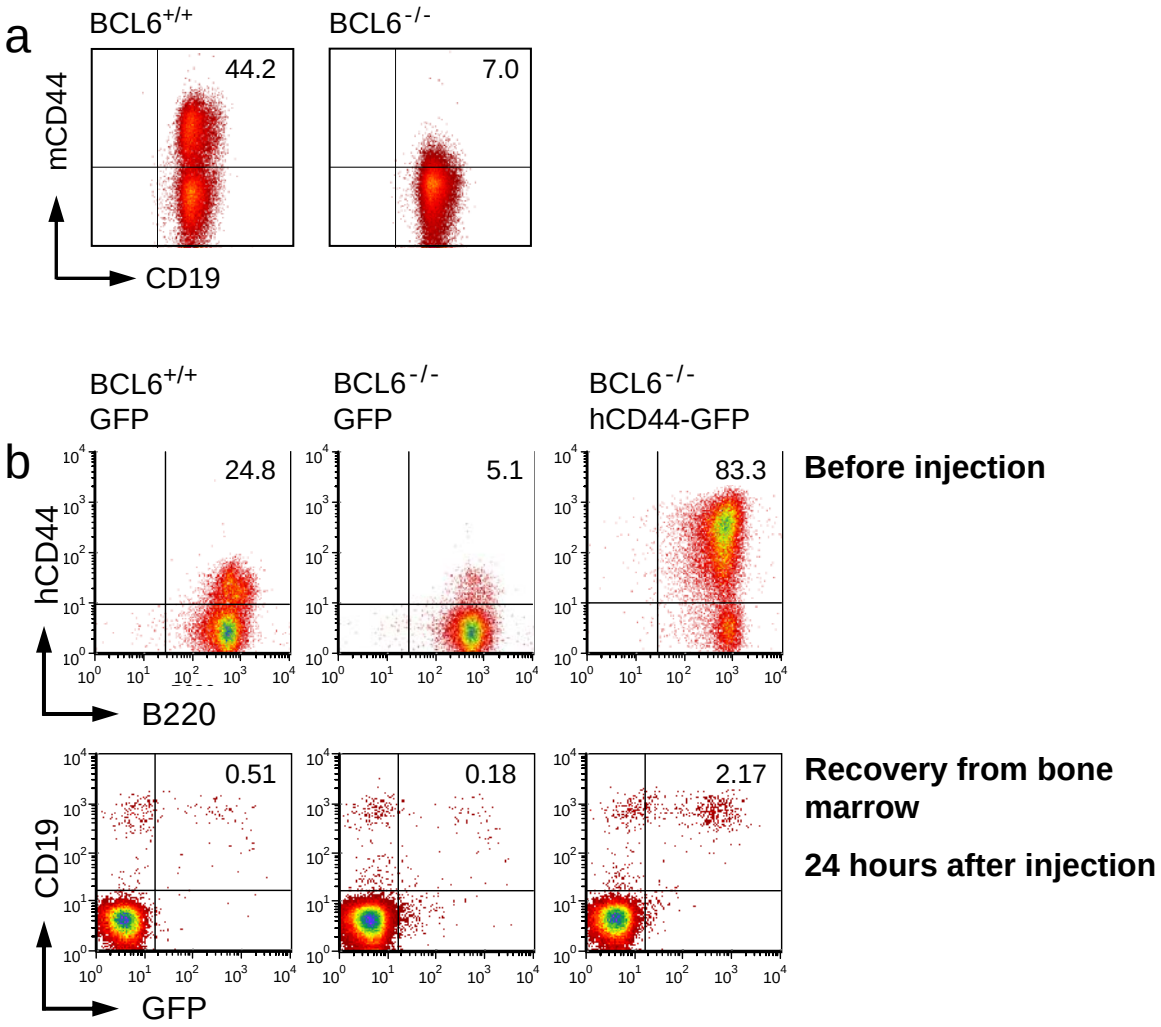

Supplementary Figure 14: *Reconstitution of CD44 in BCL6$^{-/-}$ leukemia cells rescues engraftment but not leukemia initiation*

BCL6$^{-/-}$ *BCR-ABL1* ALL cells lack expression of the homing receptor CD44 (a), which is critical for homing of leukemia-initiating cells to the bone marrow microenvironment[24]. *BCR-ABL1* ALL cells were transduced with human CD44 or an empty vector control (b). To directly address the role of CD44, we reconstituted CD44 expression in BCL6$^{-/-}$ *BCR-ABL1* ALL cells using a retroviral expression vector and determined how CD44 reconstitution affects engraftment and leukemia-initiation from BCL6$^{-/-}$ *BCR-ABL1* ALL cells. 2 x 10^6 cells were injected via tail vein. Three mice in each group were sacrificed after 24 hours and engraftment of GFP$^+$ leukemia cells in the bone marrow was measured by flow cytometry.

Consistent with lack of CD44 surface expression, recovery of BCL6$^{-/-}$ ALL cells from the bone marrow of transplant recipients was significantly reduced compared to BCL6$^{+/+}$ ALL cells 24 hours after tail vein injection (b and c; p=0.025). Retroviral reconstitution of CD44 expression increased the recovery of injected cells from the bone marrow by more than 10-fold (b-c; p<0.001). However, while overexpression of CD44 rescued homing of BCL6$^{-/-}$ *BCR-ABL1* ALL cells to the bone marrow, CD44 reconstitution failed to restore leukemia-initiation in BCL6$^{-/-}$ ALL cells (d). Hence, the failure of BCL6$^{-/-}$ ALL cells to initiate leukemia is not primarily owing to a CD44-dependent defect in homing to the bone marrow niche.

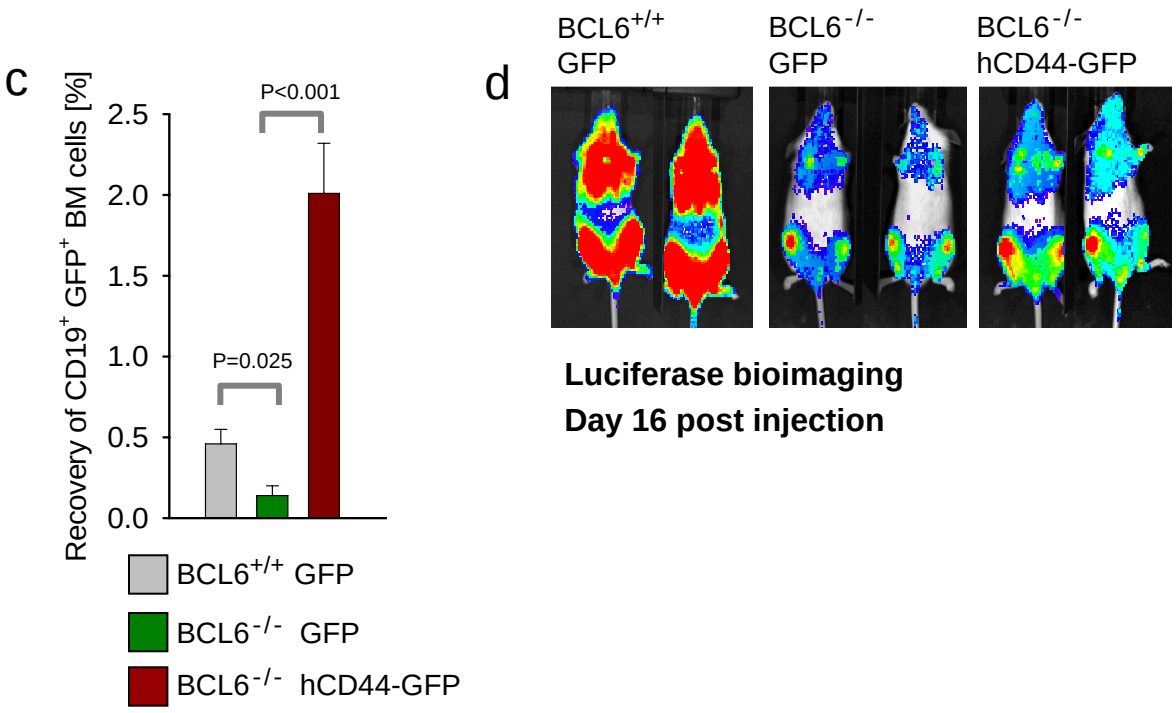

Supplementary Figure 14 continued.

In (c), the quantitative analysis of recovery of GFP^+ cells from the bone marrow of engrafted leukemia cells is summarized (n=3; means ± SD). Leukemia cells from $BCL6^{+/+}$ and $BCL6^{-/-}$ mice were labeled with firefly luciferase to track leukemia-initiation after initial engraftment of leukemia cells. Leukemia-initiation was measured 16 days after injection by luciferase bioimaging in the remaining mice (d).

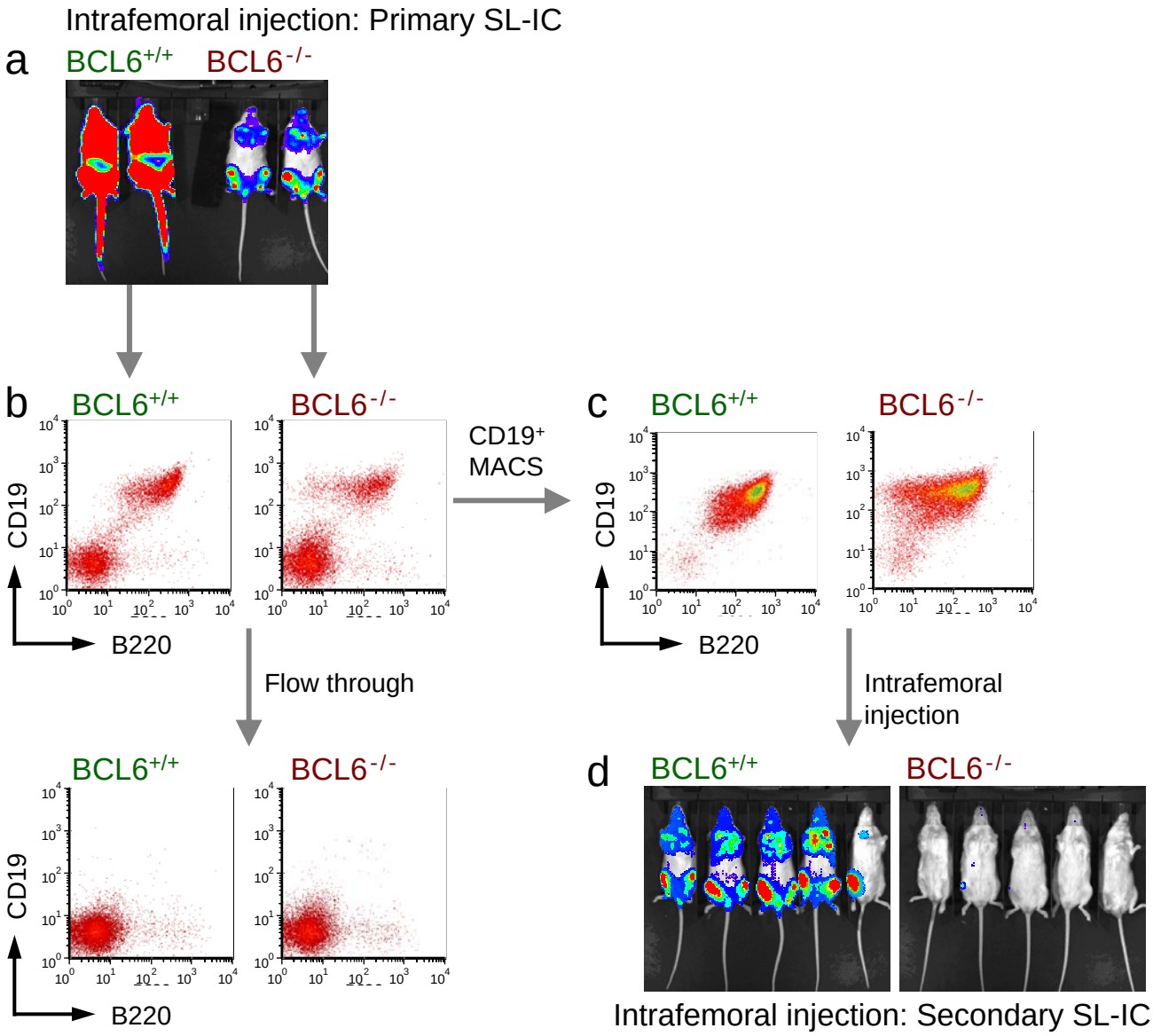

Supplementary Figure 15: *BCL6$^{-/-}$ leukemia is not transplantable in serial transplant recipients*

5,000,000 BCL6$^{+/+}$ and BCL6$^{-/-}$ BCR-ABL1-transformed ALL cells were intrafemorally injected into sublethally irradiated NOD/SCID mice (see Figure 3d). Intrafemoral injection of large numbers of leukemia cells bypasses the leukemia-initiation step: as shown by luciferase bioimaging, the mice develop leukemia soon after injection of 5,000,000 leukemia cells (a; luciferase bioimaging on day 10 after injection). Leukemia cells were harvested from ill mice and stained for expression of CD19 and B220 (b). Using CD19 MACS beads, B lymphoid leukemia cells were enriched (Example; c). 5,000,000 BCL6$^{+/+}$ and BCL6$^{-/-}$ leukemia cells were intrafemorally injected into secondary recipients. Despite the large number of intrafemorally injected cells, BCL6$^{-/-}$ leukemia was not transplantable into secondary recipients (d; luciferase bioimaging on day 8 after injection).

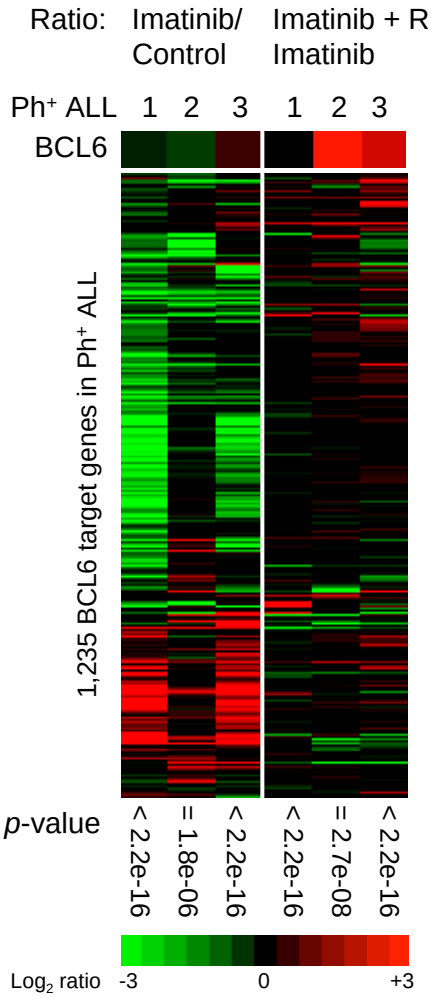

Rationale:

To determine whether RI-BPI reverses BCL6-dependent gene expression changes, we treated human *BCR-ABL1* ALL cells with Imatinib (TKI; 10 μmol/l) alone or in a combination with RI-BPI (20 μmol/l). Gene expression data (41,093 probesets) were divided into two datasets, namely known BCL6 target genes (2,956 probe sets) and Non-target genes (38,137 probe sets). If RI-BPI is a selective inhibitor of BCL6-dependent gene expression changes, we predicted that BCL6 target genes are de-repressed by RI-BPI to a significantly higher degree than Non-target genes. Indeed, we found highly significant de-repression of BCL6-targets as compared to Non-target genes (p-values ranging from $< 2.2 \times 10^{-16}$ to 2.76×10^{-8}) and conclude that RI-BPI is a potent and selective inhibitor of BCL6-dependent gene expression changes in Imatinib-treated Ph^+ ALL.

Supplementary Figure 16 : *RI-BPI reverses BCL6-dependent gene expression changes in human Ph^+ ALL cells*

Three human Ph^+ ALL cell lines were treated in the presence or absence of 10 μmol/l Imatinib or in the presence of both 10 μmol/l Imatinib and 20 μmol/l RI-BPI for 24 hours. Gene expression changes upon treatment with Imatinib or Imatinib + RI-BPI were analyzed using Agilent gene expression arrays.

Kolmogorov-Smirnov test (KS-test) to determine if two data sets differ significantly was performed. 1,235 known BCL6 target genes (covered by 2,956 probe sets) and Non-target genes (covered by 38,137 probe sets) were compared using Agilent gene expression arrays. For Imatinib vs. Control (left), we tested if BCL6 target genes have lower values (log fold change) than Non-target genes. Lower gene expression values would be consistent with BCL6-mediated repression. For Imatinib + RI-BPI vs. Imatinib (right), we tested if BCL6 target genes have higher values ($\log_2$ fold change) than Non-target genes. Higher gene expression values would be consistent with RI-BPI-mediated de-repression of BCL6-target genes. As one example, negative autoregulation of BCL6 is shown in the top row: Treatment with RI-BPI leads to transcriptional de-repression of BCL6. The bottom panel indicates *p*-values for the comparison of gene expression values for known BCL6 target genes and Non-target genes as determined by KS-test. Data are available from GEO superseries GSE24426 including GEO accession numbers GSE24381 and GSE24404.

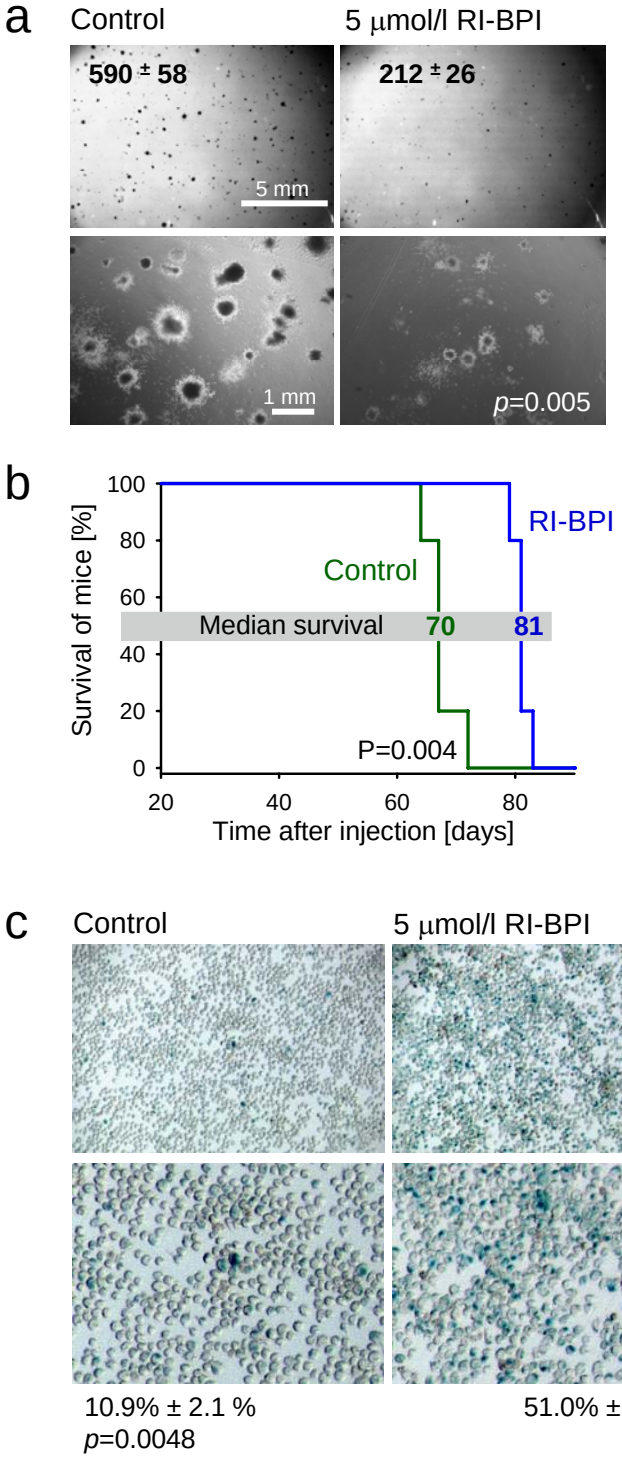

Supplementary Figure 17 : *RI-BPI compromises self-renewal and induces senescence in human Ph⁺ ALL cells*

(a) Human Ph⁺ ALL cells (10,000) were plated in semisolid agar in either the presence or absence of 5 μmol/l *retro-inverso* BCL6 peptide-inhibitor (RI-BPI). Colonies were counted after ten days (numbers denote means ± SD, n=3). **(b)**, Patient-derived Ph⁺ ALL cells (BLQ5; Supplemental Table 1) were incubated *ex vivo* for two days in the presence of RI-BPI (5 μmol/l) and injected into sublethally irradiated NOD/SCID mice. A Kaplan-Meier analysis of survival is shown (5 mice per group, p=0.004). **(c)**, Human Ph⁺ ALL cells were treated with or without 5 μmol/l *retro-inverso* BCL6 peptide-inhibitor (RI-BPI) for three days. Senescence-associated β-galactosidase (SA-β-gal) activity as an indicator of cellular senescence was measured on cytospin preparations. Percentages reflect SA-β-gal⁺ cells (means ± SD, n=3).

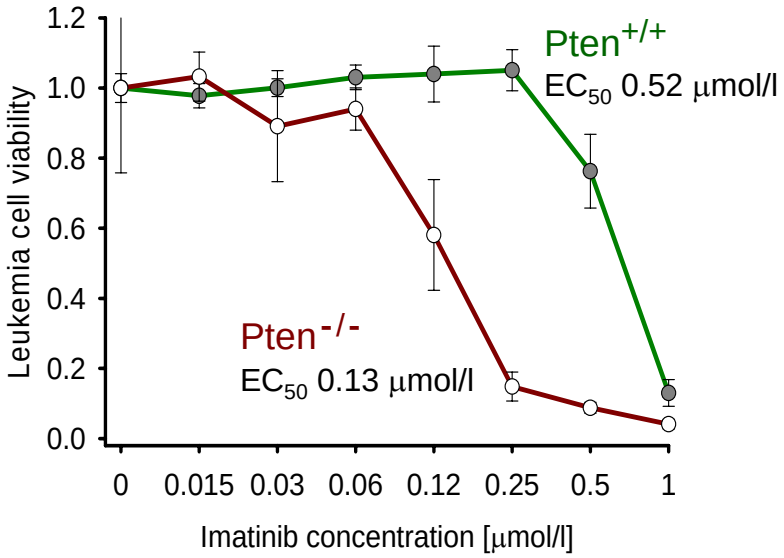

Supplementary Figure 18: *Deletion of Pten sensitizes BCR-ABL1-transformed ALL cells to TKI-treatment*

Upon inducible deletion of *Pten*, *BCR-ABL1*-transformed ALL cells lose the ability to upregulate BCL6 and Imatinib-treatment results in very high levels of p53 (see Figure 1e). Consistent with impaired ability to upregulate BCL6, inducible deletion of *Pten* results in increased sensitivity of leukemia cells to Imatinib treatment (p=0.002). Curves depict means (± SD) of triplicate measurements.

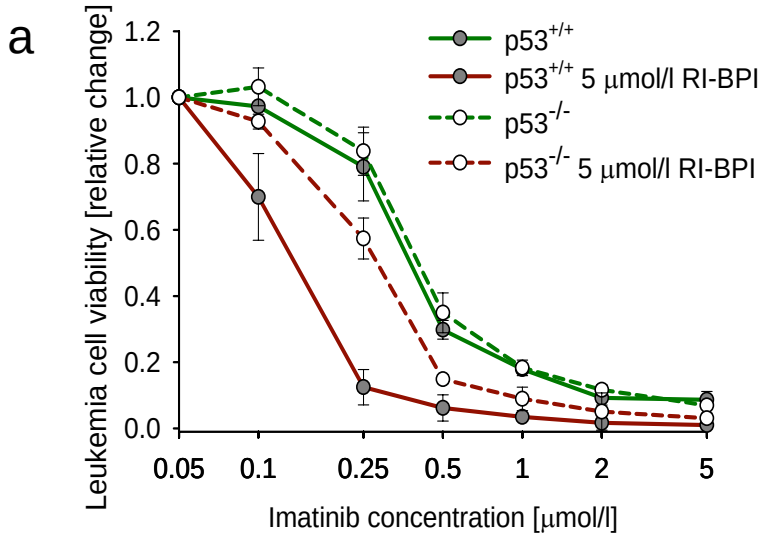

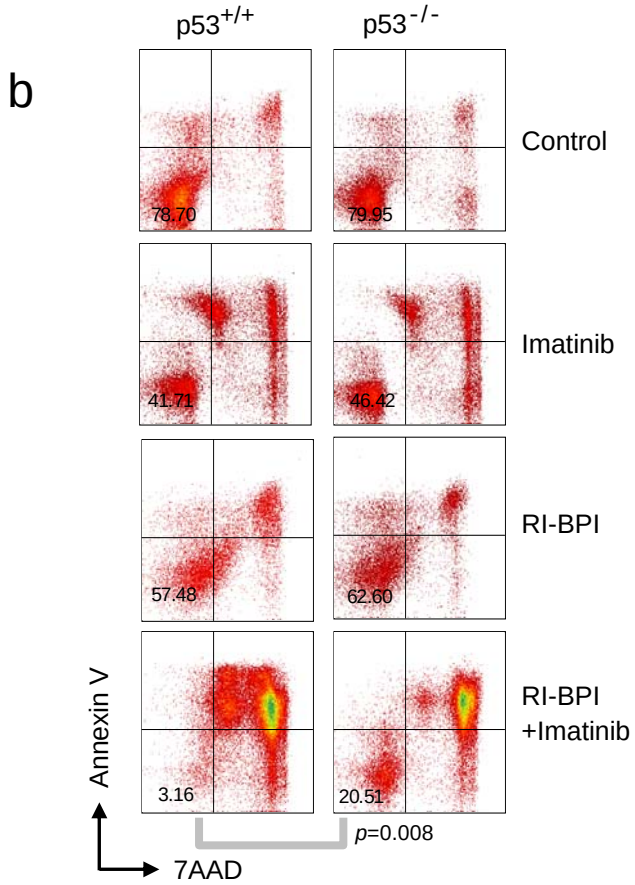

Supplementary Figure 19: *p53 is suppressed by BCL6 and contributes to Imatinib-mediated apoptosis in BCR-ABL1 ALL*

B cell precursors from $p53^{+/+}$ and $p53^{-/-}$ mice were transformed by *BCR-ABL1*. After full transformation, leukemia cells were treated with or without Imatinib or a combination of Imatinib and RI-BPI (5 µmol/l). In (**a**), drug-responses to different doses of Imatinib are measured to test whether RI-BPI sensitizes $p53^{+/+}$ and $p53^{-/-}$ leukemia cells to Imatinib (Resazurin assay). Curves denote mean values ± SD; n=3. While RI-BPI had a significant effect on $p53^{+/+}$ ALL cells, the effect of RI-BPI was reduced on $p53^{-/-}$ ALL cells. Likewise, a combination of Imatinib and RI-BPI was strongly synergistic in $p53^{+/+}$ ALL cells whereas the effect of RI-BPI was reduced on $p53^{-/-}$ ALL cells as measured by flow cytometry (**b**).

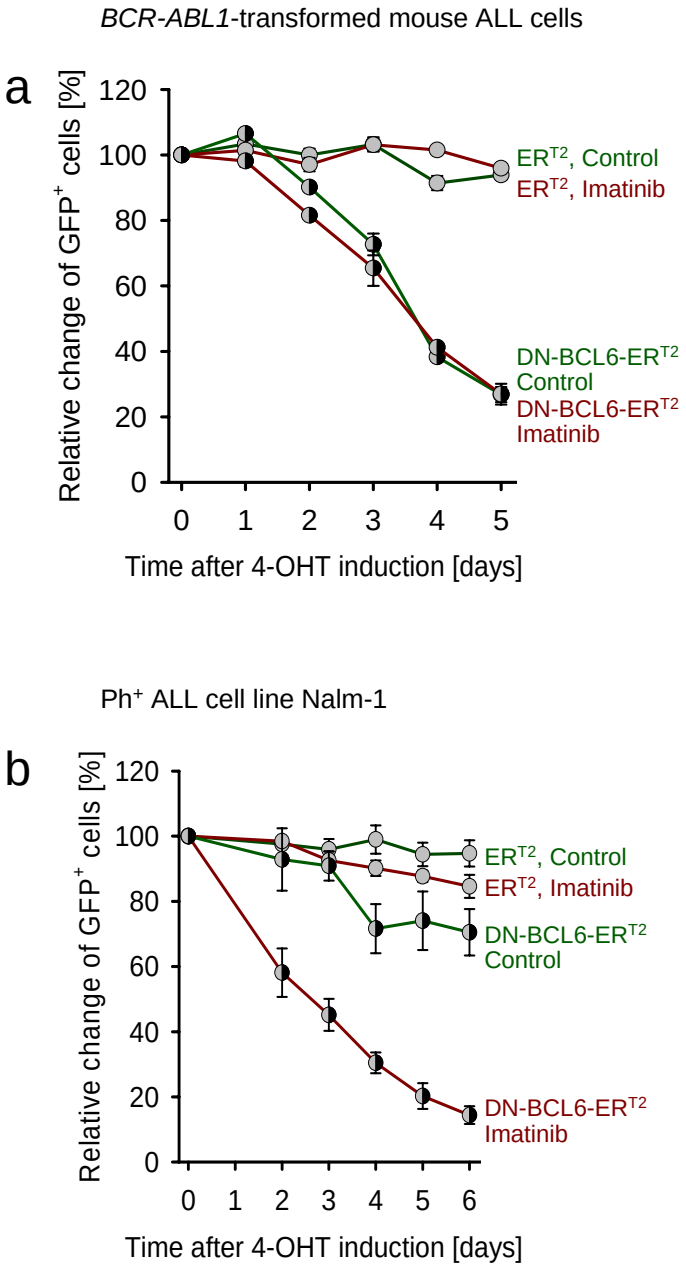

Supplementary Figure 20: *Inducible activation of a dominant-negative BCL6 mutant in BCR-ABL1-transformed ALL cells*

BCR-ABL1-transformed mouse ALL cells (pro-/pre-BI phenotype) were transduced with 4-OHT inducible dominant-negative BCL6 (DN-BCL6-ER^{T2}) or ER^{T2} empty vectors (reference 26), which are tagged with GFP (a). In a parallel experiment, a human Ph^{+} ALL cell line (Nalm1) was transduced with the same constructs (b). Mouse and human leukemia cells were then treated with or without 1 μmol/l Imatinib (mouse) or 10 μmol/Imatinib (human cell line) and DN-BCL6-ER^{T2} or ER^{T2} were induced by addition of 4-OHT. The relative changes of GFP^{+} cells after 4-OHT induction are indicated. Curves denote mean values ± SD; n=3.

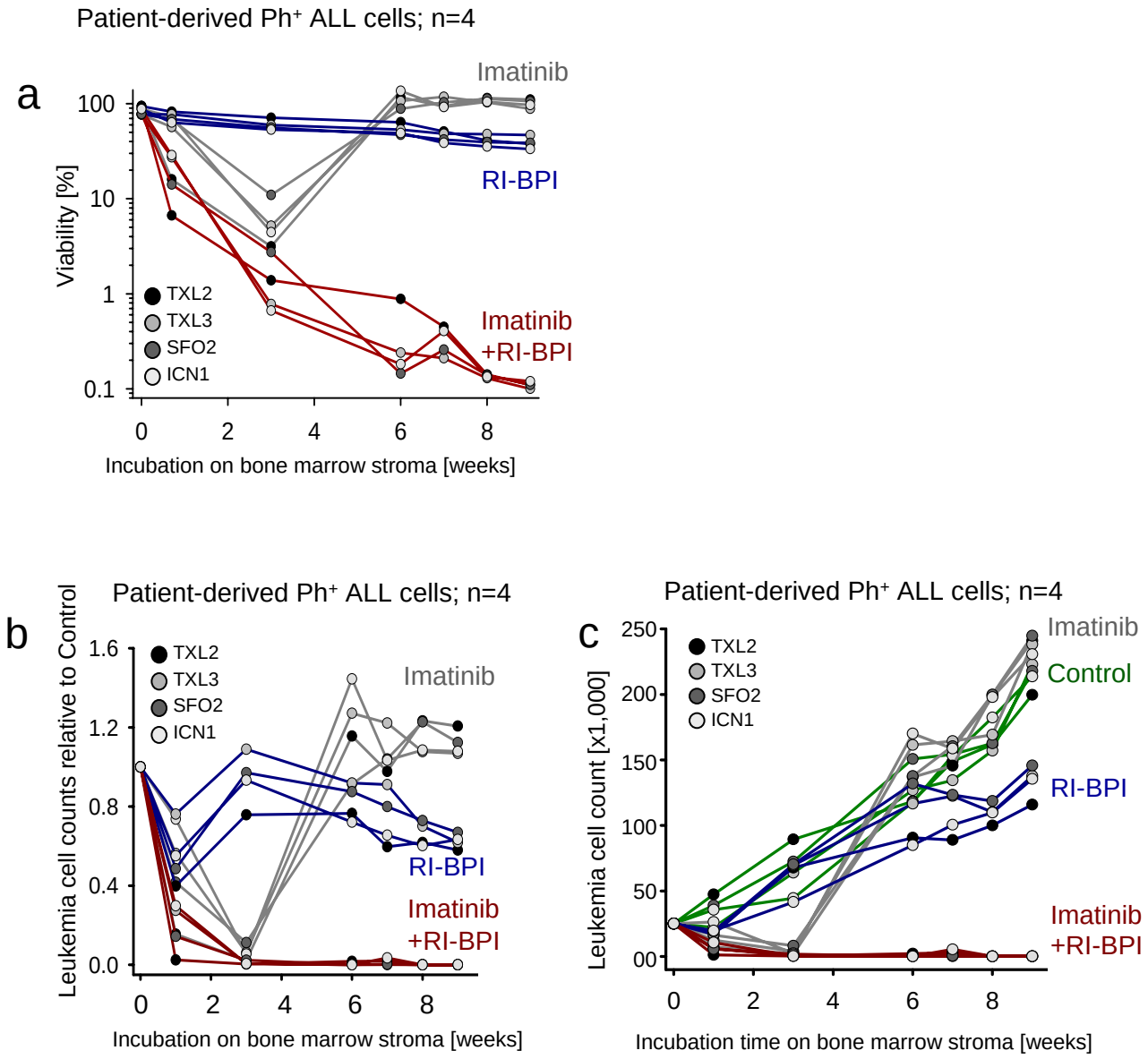

Supplementary Figure 21: *RI-BPI-mediated inhibition of BCL6 prevents outgrowth of Imatinib-resistant subclones in patient-derived Ph⁺ ALL*

Primary patient-derived Ph⁺ ALL cells from bone marrow biopsies of 4 patients (TXL2, TXL3, SFO2 and ICN1; see Table S1) were isolated and incubated on OP9 stroma cells. In all 4 cases, samples were obtained at the time of diagnosis and none of the patients was previously treated with Imatinib. Sequence analysis revealed that the BCR-ABL1 kinase domain in patient-derived ALL cells was unmutated in all 4 cases. BCR-ABL1 ALL cells were treated in the presence or absence of Imatinib (10 μmol/l) and/or RI-BPI (10 μmol/l).

After 5 days, 3 weeks, 6 weeks, 7 weeks, 8 weeks and 9 weeks, aliquots from cell cultures were analyzed by flow cytometry for cell viability (Annexin V, 7-AAD and forward scatter) and cell number. (a) Shows a synopsis of viability measurements (log scale). (b) Shows changes of cell number relative to untreated control (set as 1.0). Individual flow cytometry measurements after 5 days (c-d) and 7 weeks of incubation (e-f) are shown.

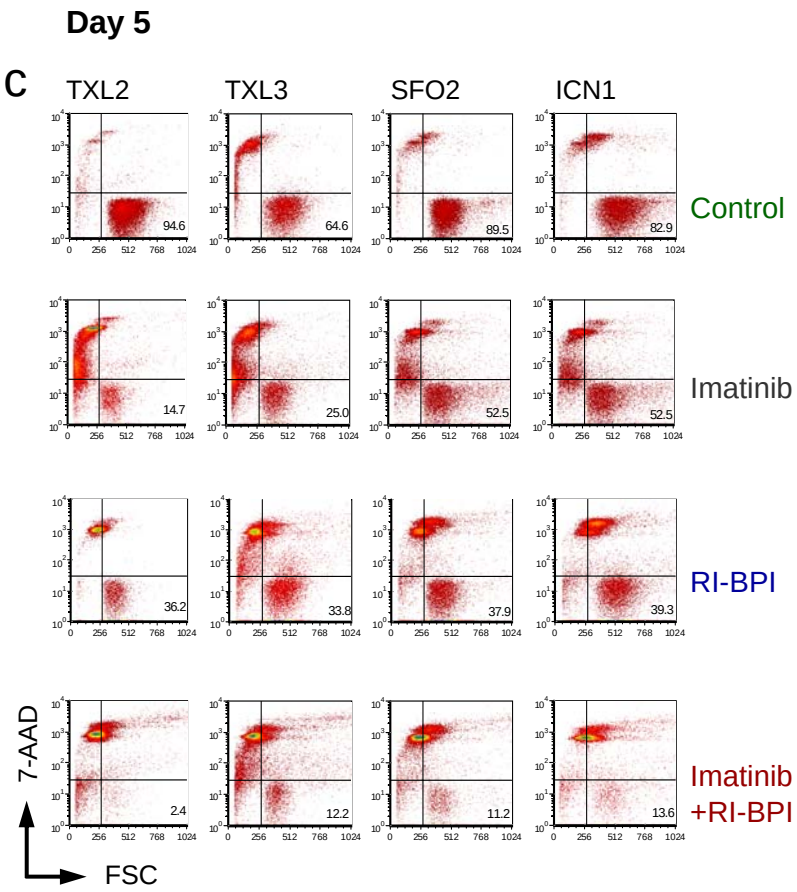

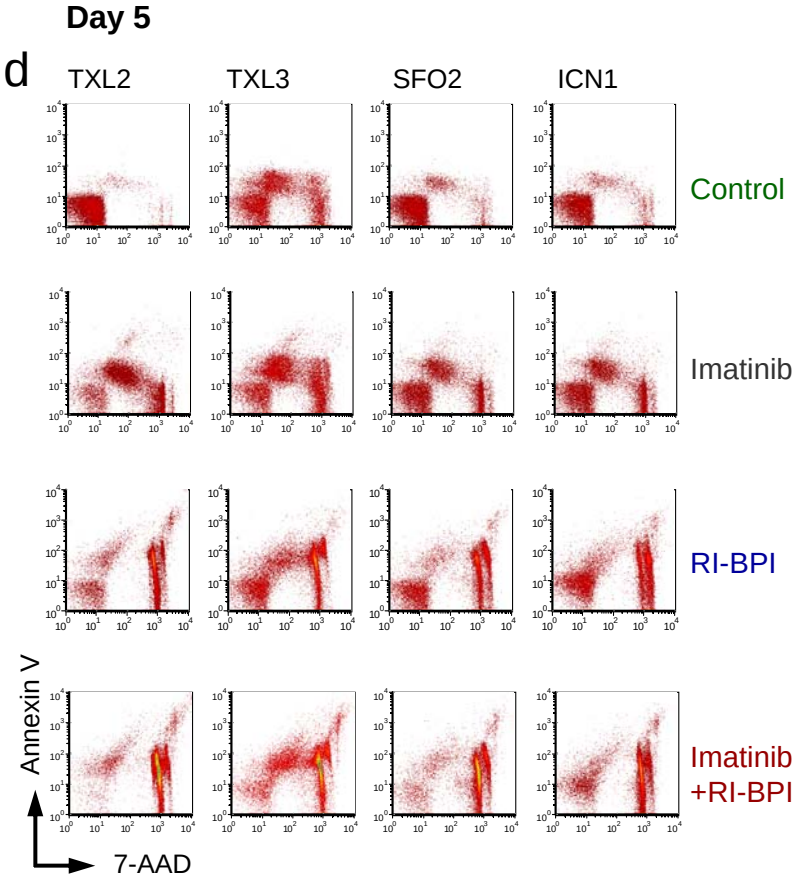

Supplementary Figure 21 (continued): *RI-BPI-mediated inhibition of BCL6 prevents outgrowth of Imatinib-resistant subclones in patient-derived Ph$^+$ ALL*

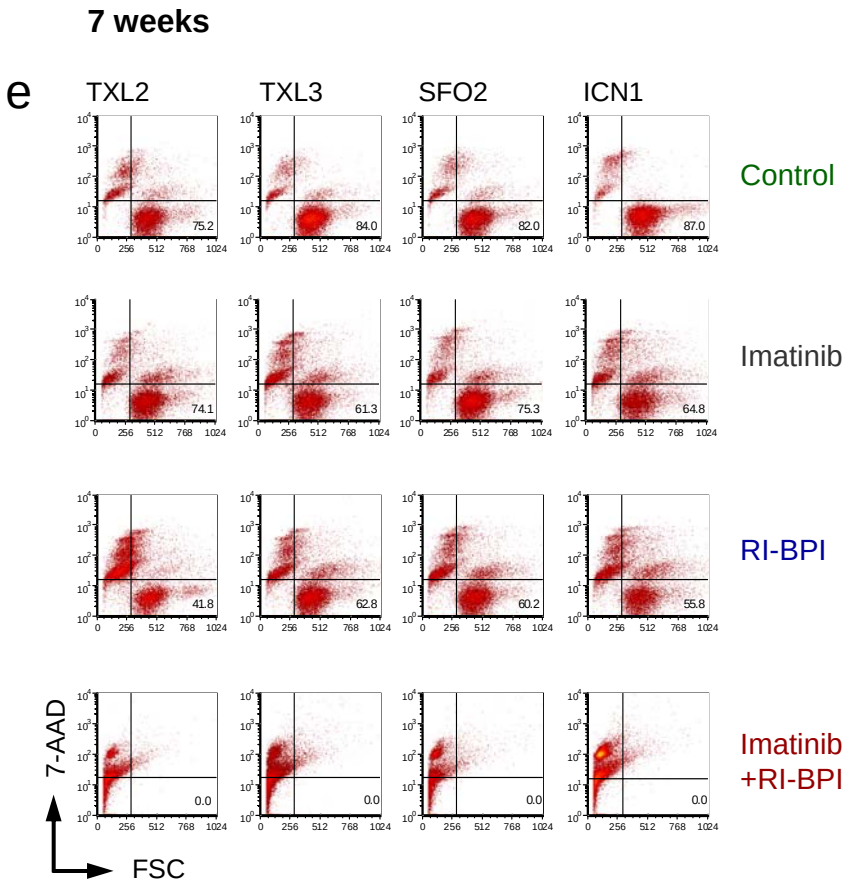

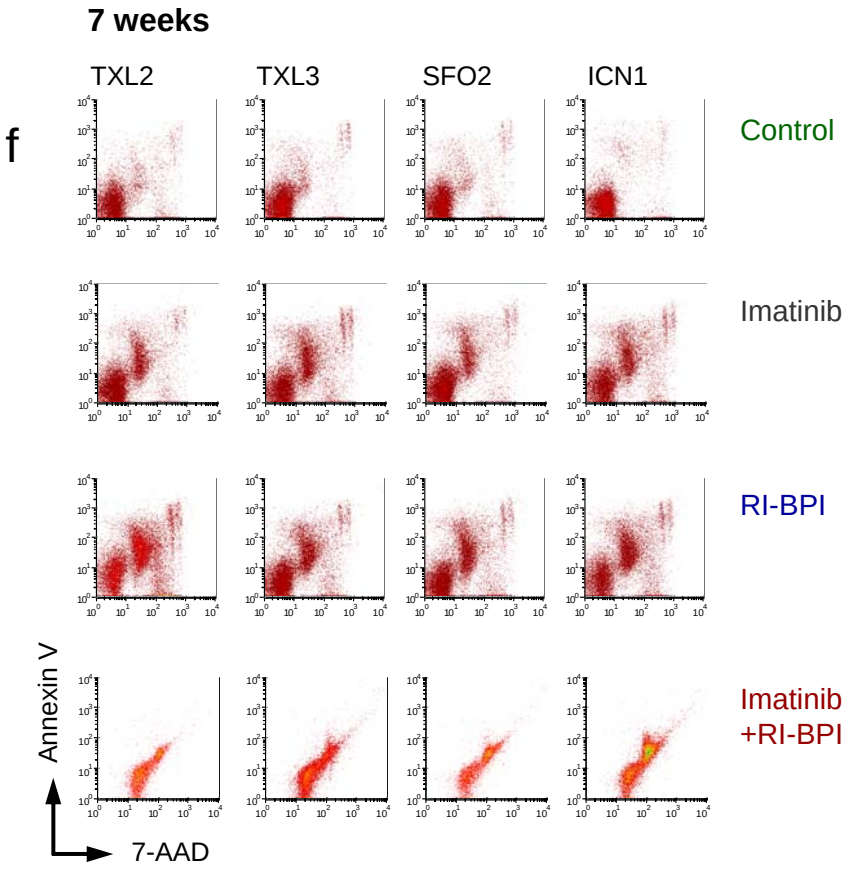

Supplementary Figure 21 (continued): *RI-BPI-mediated inhibition of BCL6 prevents outgrowth of Imatinib-resistant subclones in patient-derived Ph$^+$ ALL*

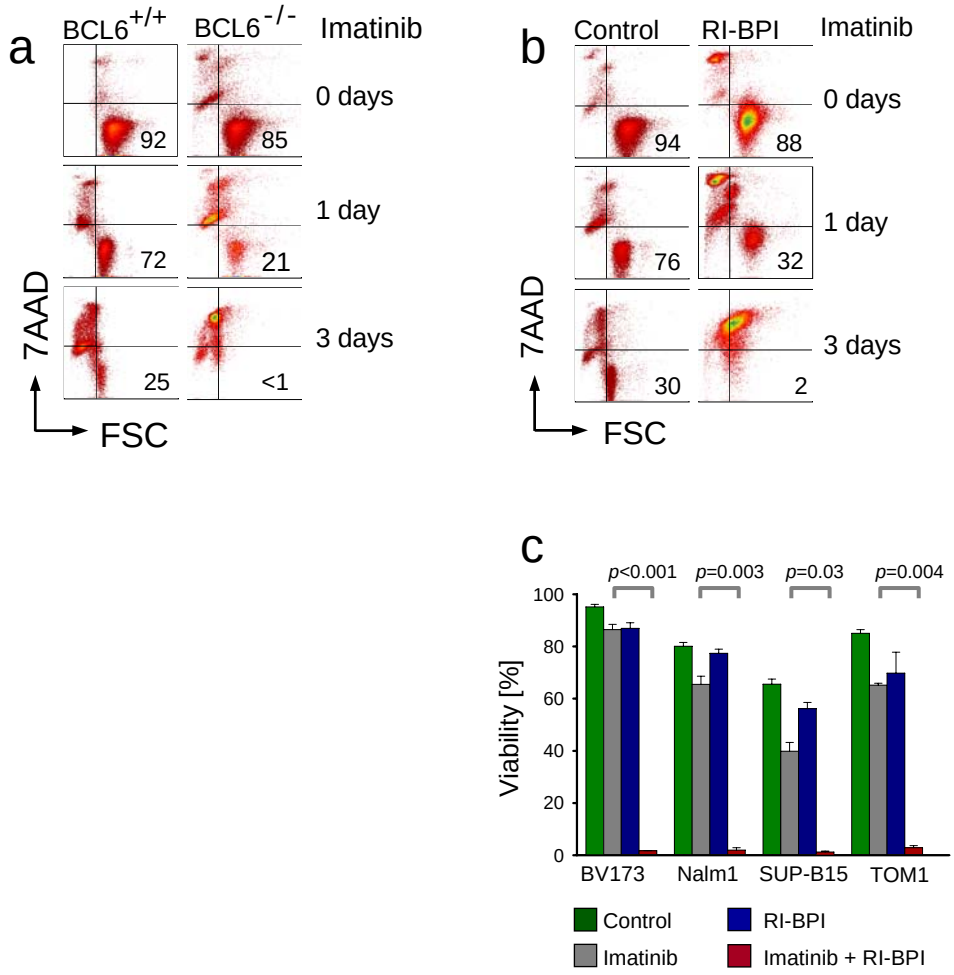

Supplementary Figure 22: *RI-BPI-mediated inhibition of BCL6 induces a similar degree of TKI-sensitivity as in BCL6$^{-/-}$ leukemia cells*

B cell precursors from BCL6$^{+/+}$ and BCL6$^{-/-}$ mice were transformed by *BCR-ABL1*. After full transformation, leukemia cells were treated with or without Imatinib (a) or a combination of Imatinib and 5 µmol/l RI-BPI (b) and viability was analyzed by flow cytometry using 7AAD and forward scatter (FSC) parameters. Likewise, four human Ph^{+} ALL cell lines (BV173, Nalm1, SUP-B15 and TOM1) were treated with or without 10 µmol/l Imatinib or with or without RI-BPI (20 µmol/l) and viability was measured after three days of treatment (c). Means (± SD) of triplicate measurements are indicated for each cell line. *p*-values were calculated for the differences between Imatinib only and Imatinib + RI-BPI combinations (double-sided t-test).

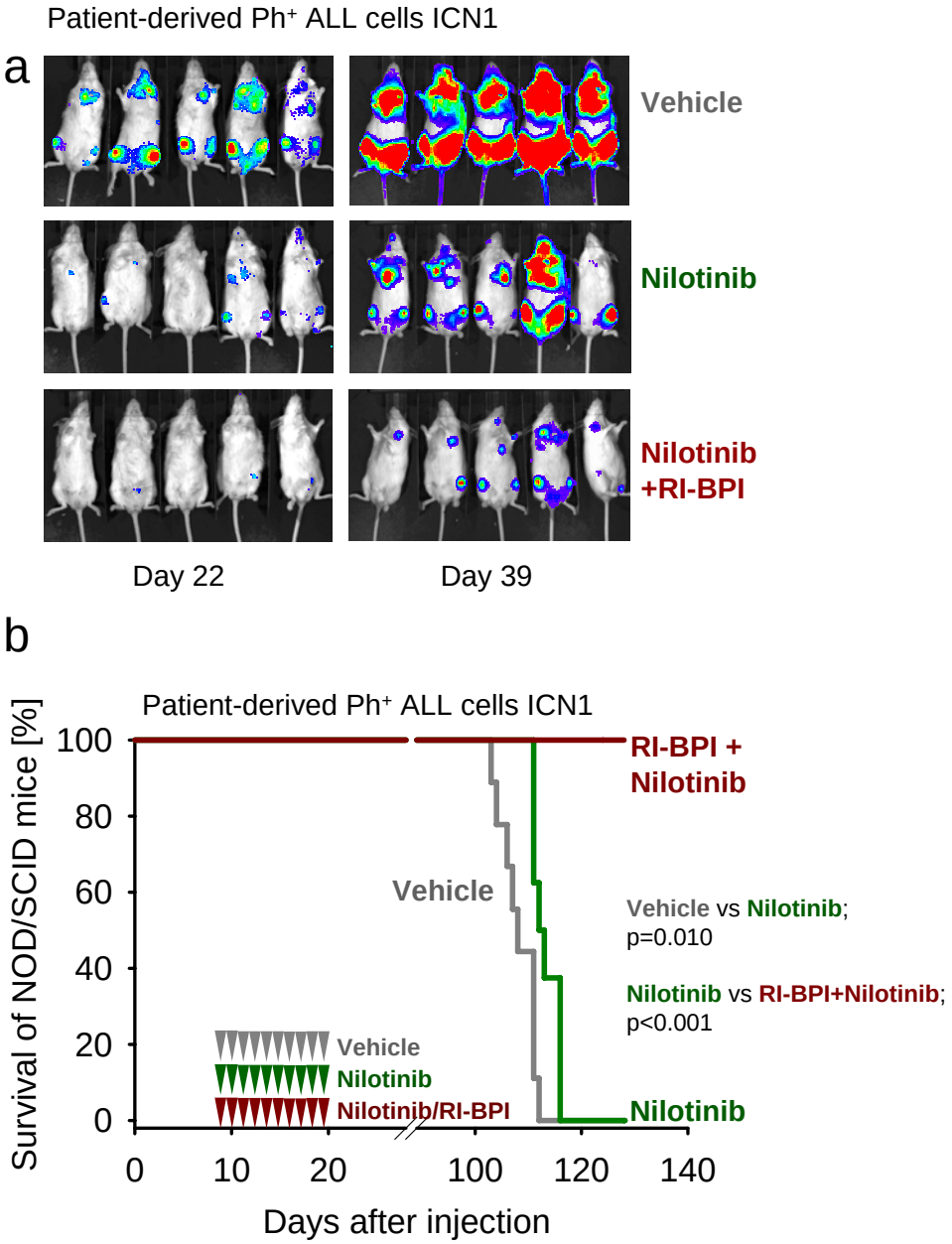

Supplementary Figure 23: *BCL6 peptide inhibition sensitizes patient-derived Ph⁺ ALL to TKI-treatment in vivo*

(a) Leukemia cells from a bone marrow biopsy of a patient with Ph⁺ ALL (ICN1, Table S1) were xenografted into sublethally irradiated NOD/SCID mice via tail vein injection. After first passage in mice, leukemia cells were harvested and transduced with lentiviral firefly luciferase and 100,000 transduced leukemia cells were injected into sublethally irradiated secondary NOD/SCID recipients. The mice were treated with daily injections of vehicle, Nilotinib (50 mg/kg) alone or Nilotinib (50 mg/kg) and RI-BPI (25 mg/kg) over a period of 10 days (days 8 to 17). Luciferase bioimaging on days 22 and 39 showed that co-treatment with RI-BPI delayed leukemia formation. (b) A Kaplan Meier-analysis of survival of mice in the three groups is shown. Arrowheads depict times of treatment.

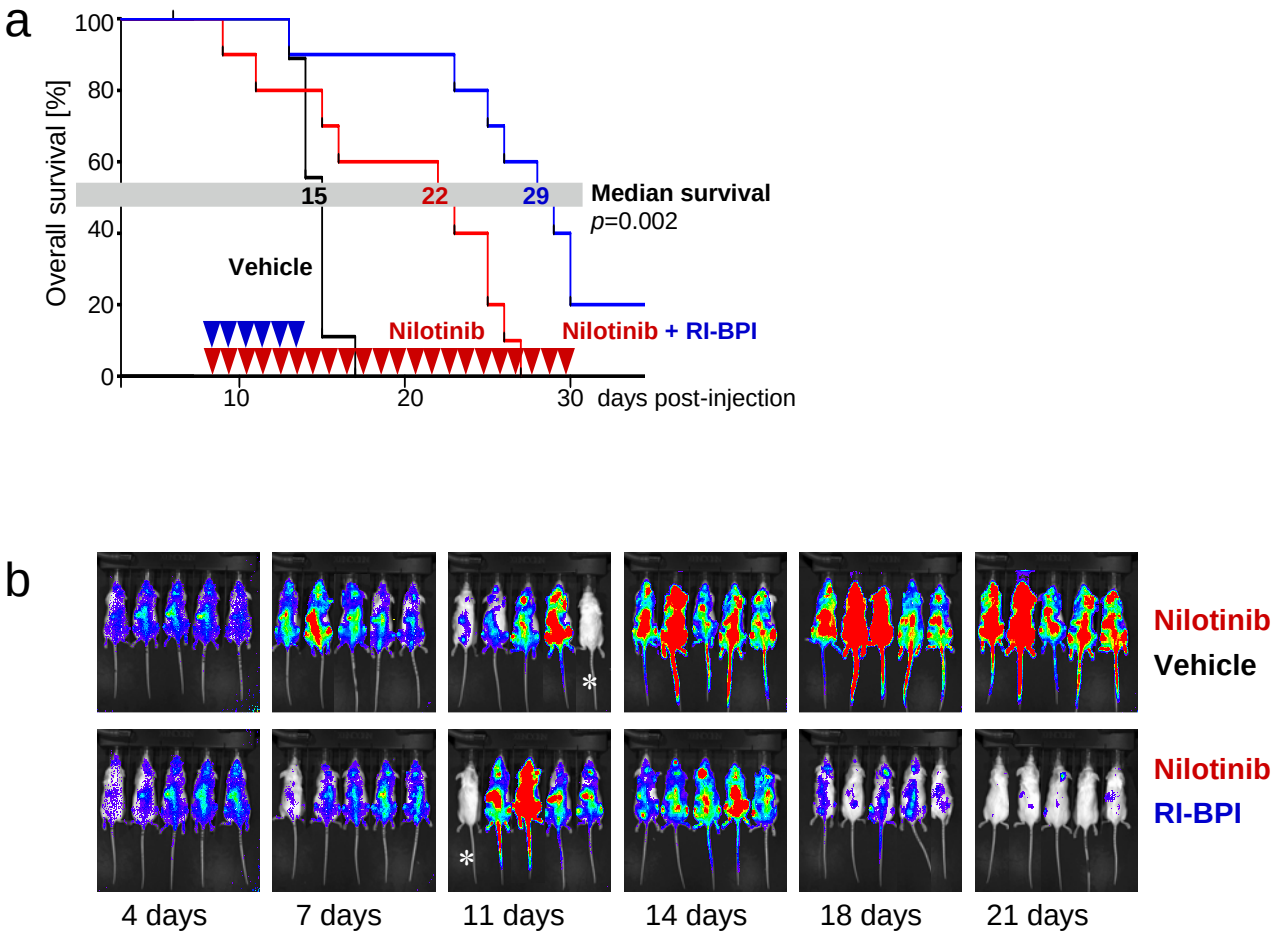

Supplementary Figure 24: *RI-BPI plus Nilotinib combination reduces disease burden in mice with full-blown leukemia*

1 x 10^6 mouse *BCR-ABL1* ALL cells were labeled with lentiviral firefly luciferase and injected into NOD/SCID mice. 4 days after injection, the first signs of engraftment were observed by luciferase bioimaging. Mice were treated six times starting on day 8 after leukemia cell injection with either the second generation TKI Nilotinib alone (25 mg/kg; red arrow heads) or a combination of Nilotinib and RI-BPI (20 mg/kg; blue arrow heads). After day 13, treatment with RI-BPI was discontinued and mice were treated daily with Nilotinib only. A Kaplan-Meier analysis of survival of mice treated with vehicle, Nilotinib alone or a combination of Nilotinib and RI-BPI (days 8-13) is shown (**a**). The kinetics of leukemia engraftment, progression and reduction of leukemia cell burden in case of Nilotinib + RI-BPI-treatment are shown by luciferase bioimaging (**b**). Asterisks denote mice with misinjections of D-luciferin.

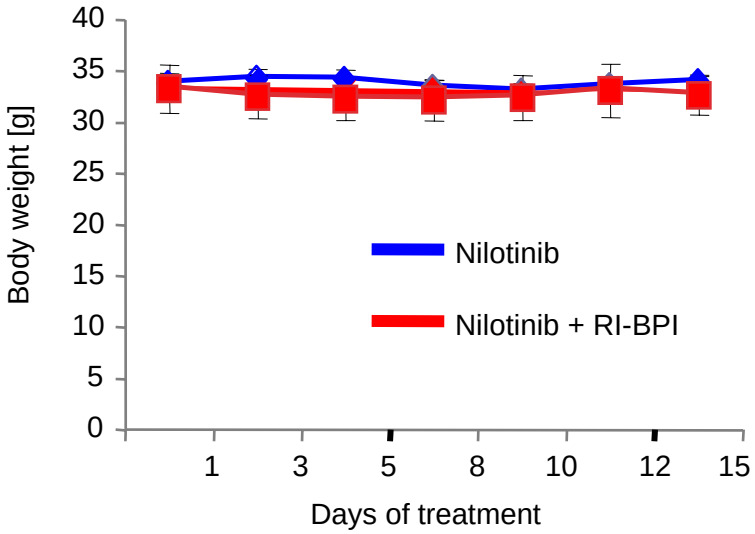

Supplementary Figure 25: *In vivo toxicology studies for Nilotinib/RI-BPI combinations -Body weight*

Ten adult C57BL/6 mice were exposed to intraperitoneal administration of RI-BPI 20 mg/kg of body weight 3 times a week (mean values ± SD; n=5) or RI-BPI 20 mg/kg of body weight 3 times a week plus Nilotinib 25 mg/kg of body weight 3 times a week by oral gavage (mean values ± SD; n=5). Five additional mice were treated with vehicle for control. One mouse in the combination group was excluded for analysis due to a severe bite wound with infection that required additional treatment. No toxic effect, such as lethargy, weight loss (see above), failure to thrive or any other indicator of sickness or organ damage, was noted with either treatment schedule. Complete blood counts showed no alteration of leukocyte, platelet and erythrocyte numbers. One mouse in the combination group presented a low hematocrit value due to intraperitoneal bleeding as consequence of the IP injection. Bone marrow examination (smear) and peripheral blood examination showed normal cell morphology. There were no alterations in the biochemistry parameters for liver function, kidney function and electrolytes (see Table S2).

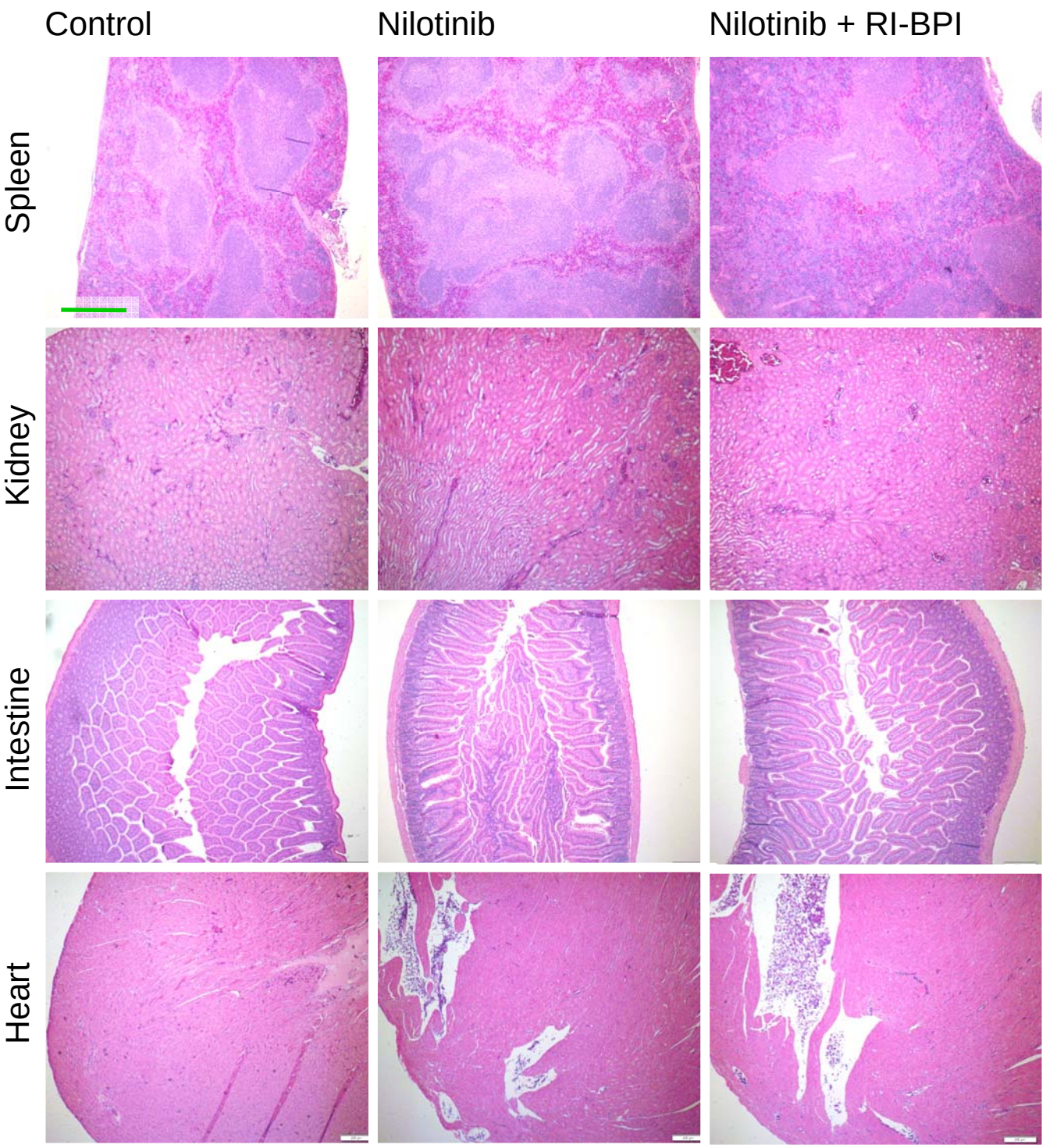

Note: Line represents 400 µm

Supplementary Figure 26: *In vivo toxicology studies for Nilotinib/RI-BPI combinations - Histology*

Representative microphotographs from the several tissues (spleen, kidney, intestine, heart, pancreas, lung, liver and bone marrow) harvested from vehicle, Nilotinib and Nilotinib+RI-BPI treated animals for toxicity assessment. Pictures were taken using a digital camera (Olympus DP72, Olympus Corp, Tokyo, Japan) attached to a light microscope (Axioskop, Carl Zeiss Crop., Maple Grove, MN) with 4x and 20x Plan Neofluar objectives (Carl Zeiss Crop., Maple Grove, MN).

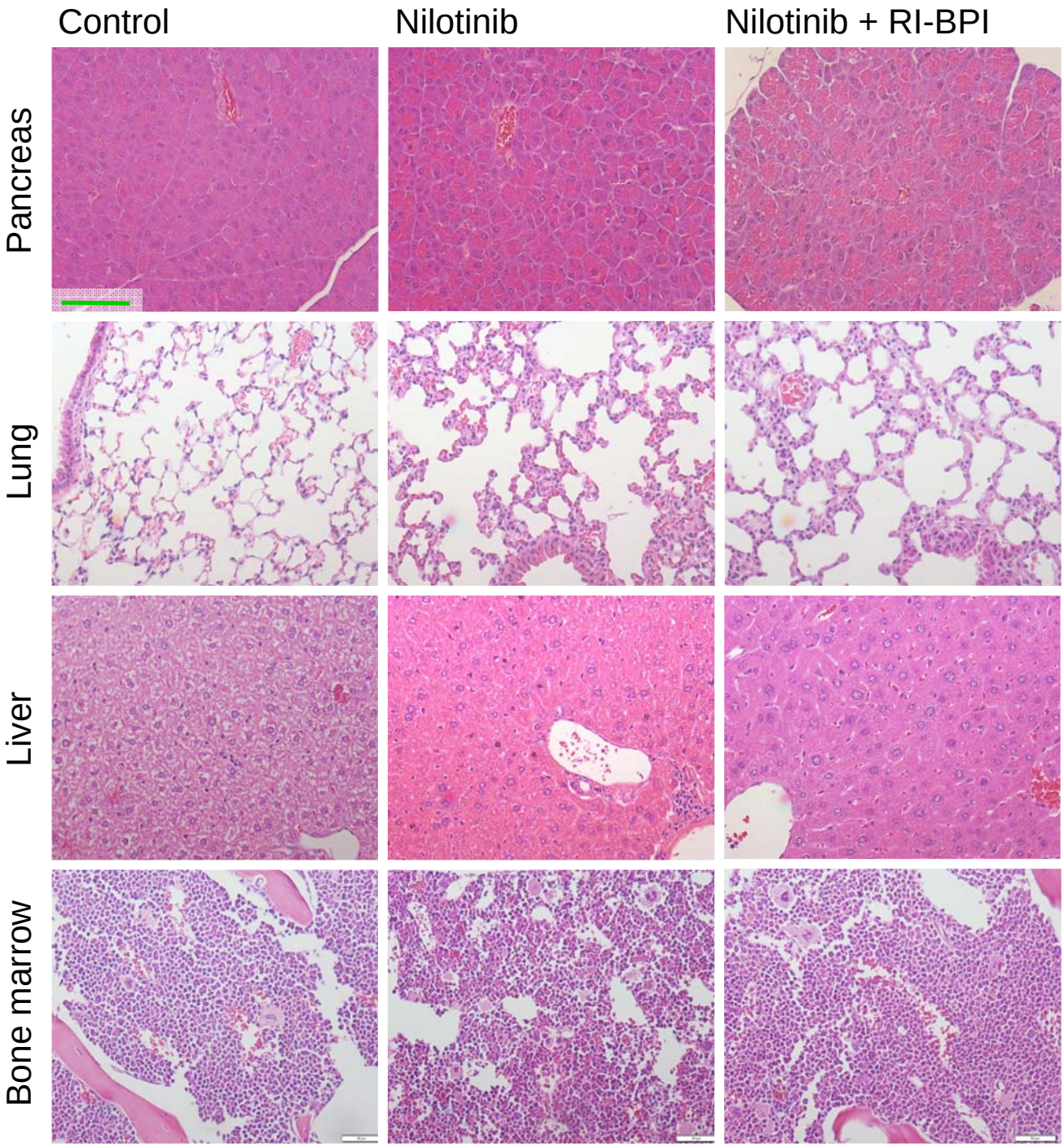

Note: Line represents 100 μm

Supplementary Figure 26 (continued): *In vivo toxicology studies for Nilotinib/RI-BPI combinations - Histology*

Supplemental Table 1: *Overview over patient-derived samples of Ph$^+$ ALL and Ph$^+$ ALL cell lines*

Case	Cytogenetics	*BCR-ABL1*	Sequence analysis	Clinical course	Gender/Age
Primary cases					
LAX2	t(9;22)(q34;q11)	p210	T315I	Relapse (Imatinib)	m/38
LAX9	t(9;22)(q34;q11) del(12)(p12;p13) del(11)(q23)	p190	unmutated	at diganosis	m
SFO2	t(9;22)(q34;q11)	p210	unmutated	at diagnosis and Relapse (Nilotinib)	m/7 m/8
BLQ1	FISH der(9), der(22)	p210	T315I	Relapse (Imatinib)	
BLQ4	FISH der(9), der(22)	p210	unmutated-	Relapse (Imatinib)	f
BLQ5	FISH der(9), der(22)	p190	T315I	Relapse (Imatinib)	f
BLQ6	FISH der(9), der(22)	n.d.	n.d.	Relapse (Imatinib)	m
BLQ11	FISH der(9), der(22)	p210	T315I	Relapse (Imatinib)	m
TXL1	t(9;22)(q34;q11)	n.d.	unmutated	at diagnosis	m/19
TXL2	t(9;22)(q34;q11)	p210	unmutated	at diagnosis	
TXL3	t(9;22)(q34;q11)	p210	unmutated	at diagnosis	
TXL4	t(9;22)(q34;q11)	n.d.	unmutated	at diagnosis	f/56
ICN1	t(9;22)(q34;q11)	p210	unmutated	at diagnosis	
ICN10	der(9)(q10)t(9;22)(q34;q11) der(22) t(9;22)(q34;q11)	n.d.	n.d.	at diagnosis	f
Cell lines					
BV173	add(1)(q42), add(8)(p23), der(22)t(9;22)(q34;q11)	p210	unmutated	B lymphoid blast crisis	m/45
Nalm1	der(7)t(7;9;15)(q10;?;q15), t(9;9)(p24;q33-q34) t(9;22) (q34;q11), der(15)t(7;9;15)	p210	unmutated	B lymphoid blast crisis	f/3
SUP-B15	t(1;1)(p11;q31), add(3)(q27), der(4)t(1;4)(p11;q35), add(10)(q25), t(9;22)(q34;q11)	p190	unmutated	Relapse	m/9
TOM1	del(7)(p14),der(9)del(9)(q13q34) der(22)t(9;22)(q34;q11)	p190	unmutated	Refractory	f/54

Notes: All primary samples are bone marrow biopsies, blast content >80%; LAX, Los Angeles; BLQ, Bologna; TXL, Berlin; SFO, San Francisco; ICN, Seoul; n.d., not done; f, female; m, male

Supplemental Table 2: *In vivo toxicology studies for Nilotinib/RI-BPI combinations, biochemistry parameters for liver, kidney function and electrolytes*

	Nilotinib		**Nilotinib + RI-BPI**			
Parameter	*Mean (n = 5)*	*SEM*	*Mean (n = 4)*	*SEM*	*Reference values*	
White blood cells	5.34	0.77	6.89	0.62	3.5-12	K/μL
Red blood cells	8.53	0.26	7.06	0.44	8.2-10.4	M/μL
Platelets	974.40	103.25	1112.75	194.84	799-1300	K/μL
WBC morphology	normal		normal			
RBC morphology	normal		normal			
Platelets morphology	normal		normal			
ALP	39.80	1.62	50.50	13.28	23-181	IU/L
GGT	0.20	0.20	0.50	0.50	0-2	IU/L
Albumin	2.54	0.07	2.28	0.05	2.5-3.9	g/dL
Total Protein	4.46	0.11	4.13	0.20	4.1-6.4	g/dL
Globulin	1.92	0.09	1.85	0.16	1.3-2.8	g/dL
Total Bilirubin	0.36	0.02	0.25	0.03	0-0.3	mg/dL
Blood Urea Nitrogen	19.60	2.18	28.00	5.37	14-32	mg/dL
Creatinine	0.14	0.02	0.10	0.00	0.1-0.6	mg/dL
Cholesterol	77.20	1.85	64.50	4.11	74-190	mg/dL
Glucose	293.00	28.18	190.25	46.97	76-222	mg/dL
Calcium	8.48	0.04	8.58	0.09	7.6-10.7	mg/dL
Phosphorus	6.78	0.47	9.03	0.99	4.6-9.3	mg/dL
Bicarbonate	21.00	1.22	19.75	1.65	11-18	mEq/L
Chloride	110.40	0.51	113.75	1.18	103-115	mEq/L
Potassium	4.92	0.27	4.93	0.34	3.4-5.5	mEq/L
Sodium	148.80	0.97	151.50	0.96	146-155	mEq/L
Osmolality	309.20	2.06	311.50	1.31	300-330	mOsm/kg

Note: Single-agent treatment with 20 mg/kg RI-BPI was recently evaluated over a period of one year (weekly injections over 52 weeks) and found to be non-toxic in mice (reference 25).

Supplemental Table 3: *Overview over mouse strains used in this study*

Mouse strain	Source	Purpose
[a]*BCL6*$^{-/-}$	Riccardo Dalla-Favera, Columbia University	Genetic loss-of-function experiments
[b]*Pten*$^{fl/fl}$	Hong Wu, UCLA	Inducible deletion of *Pten* (FoxO inactivation)
[c]*Stat5*$^{fl/fl}$	Lothar Hennighausen, NIDDK	Inducible deletion of *Stat5a* and *Stat5b*
NOD/SCID	Jackson Laboratories	Xenograft recipient mice
Trp53$^{-/-}$	Jackson Laboratories	Analysis of p53 as BCL6 target gene

Notes:

a Ye BH, Cattoretti G, Shen Q, Zhang J, Hawe N, de Waard R, Leung C, Nouri-Shirazi M, Orazi A, Chaganti RS, Rothman P, Stall AM, Pandolfi PP, Dalla-Favera R. The BCL-6 proto-oncogene controls germinal-centre formation and Th2-type inflammation. *Nat Genet.* 1997; 16: 161-70.

b Groszer M, Erickson R, Scripture-Adams DD, Lesche R, Trumpp A, Zack JA, Kornblum HI, Liu X, Wu H. Negative regulation of neural stem/progenitor cell proliferation by the Pten tumor suppressor gene in vivo. *Science*. 2001; 294: 2186-9.

c Liu X, Robinson GW, Wagner KU, Garrett L, Wynshaw-Boris A, Hennighausen L. Stat5a is mandatory for adult mammary gland development and lactogenesis. *Genes Dev*. 1997; 11: 179-86.

Supplemental Table 4: *Sequences of oligonucleotide primers used*

Quantitative RT-PCR

Human

*BCL6*_F	5'-CTCAGATTCTAGCTGTGAGAACG-3’
*BCL6*_R	5'-GTCACACTTGTAGGGTTTGTCAC-3’
*COX6B*_F	5'-AACTACAAGACCGCCCCTTT-3'
*COX6B*_R	5'-GCAGCCAGTTCAGATCTTCC-3'

Mouse

*Bcl6*_F	5’-CCTGCAACTGGAAGAAGTATAAG-3’
*Bcl6*_R	5’-AGTATGGAGGCACATCTCTGTAT-3’
*Cdkn2a*_F	5’-GGACCAGGTGATGATGATG-3’
Cdkn2a _R	5’-ATCGCACGATGTCTTGATG-3’
Cdkn1a _F	5’-ACAAGAGGCCCAGTACTTC-3’
*Cdkn1a*_R	5’-CTTGCAGAAGACCAATCTG-3’
Cdkn1b _F	5’-GTGTCCAGGGATGAGGAAG-3’
*Cdkn1b*_R	5’-CGGAGCTGTTTACGTCTGG-3’
*Trp53*_F	5’-TCCTTACCATCATCACACTGG-3’
*Trp53*_R	5’-CGGATCTTGAGGGTGAAATAC-3’
*Hprt*_F	5’-GGGGGCTATAAGTTCTTTGC-3’
*Hprt*_R	5’-TCCAACACTTCGAGAGGTCC-3’

Quantitative chromatin immunoprecipitation (Q-ChIP)

*CDKN2A*_F	5’-GCGTGCAGCGGTTTAGTTTA-3’
*CDKN2A*_R	5’-TCAGGAGGCTGAATGTCAGTT-3’
*CDKN1B*_F	5’-TACAATCCCGGGAAAGAACA-3’
*CDKN1B*_R	5’-GATCTTCCTTCCCAAGCACA-3’

Clonality and spectratyping analysis

V_H1_F	5'-AAGGCCACACTGACTGTAGAC-3'
J_H2_R	5'-GAGGAGACTGTGAGAGTGGTG-3'
Cμ_R	5'-TGGCCACCAGATTCTTATCAG-3'
J_H1-FAM_R	5'-GACGGTGACCGTGGTCCCTGT-3'
J_H2-FAM_R	5'-GACTGTGAGAGTGGTGCCTTG-3'
J_H3-FAM_R	5'-GACAGTGACCAGAGTCCCTTG-3'
J_H4-FAM_R	5'-GACGGTGACTGAGGTTTCTTG-3'
Cμ-FAM_R	5'-AGACGAGGGGGAAGACATTTG-3'

Notes: V_H1_F binds to rearranged V_H gene segments of the J558 family. FAM denotes dye-labeled oligonucleotide. The label is attached to the 5' end.

Supplemental Table 5: *Summary of accession numbers for gene expression, ChIP-on-chip and CGH data*

GEO accession	GEO description	Results	Figure
GSE23743	Effect of Imatinib on Ph^+ acute lymphoblastic leukemia	Gene expression result from human Ph^+ ALL	Supplemental Figure 2a, Supplemental Figure 3
GSE24426	SuperSeries composed of GSE24381 and GSE24404; GSE24381: Inhibition of BCL6-dependent gene expression in Ph^+ acute lymphoblastic leukemia; GSE24404: Recruitment of BCL6 to target genes in Ph^+ acute lymphoblastic leukemia	GSE24381 (BCL6-dependent gene regulation in Ph^+ ALL); GSE24404 (ChIP-on-chip of BCL6 in Ph+ ALL)	Figure 2b, Supplemental Figure 9, Supplemental Figure 11 Supplemental Figure 16
GSE15179	ChIP-on-chip analysis of BCL6-DNA interactions	ChIP-on-chip data from BCL6 in lymphoma (OCI-LY1 and OCI-LY7)	Figure 2b Supplemental Figure 9
GSE11794	Untreated 32Dcl3 cell lines expressing oncogenic tyrosine kinases or cells treated with small molecule inhibitors	Gene expression result from the 32Dcl3 cell line with oncogenic tyrosine kinases	Supplemental Figure 2a, Supplemental Figure 3
GSE10086	Expression profiling of ^{V600E}BRAF and RTK-activated cells upon MEK inhibition	Gene expression result from solid tumor cell lines	Supplemental Figure 3
GSE20987	Gene expression data of BCR-ABL1 transformed B cell precursors from $BCL6^{+/+}$ and $BCL6^{-/-}$ mice	Gene expression result from $BCL6^{+/+}$ and $BCL6^{-/-}$ BCR-ABL1 ALL	Supplemental Figure 6
GSE24400	Comparison of copy number variations between $BCL6^{+/+}$ and $BCL6^{-/-}$ BCR-ABL1-driven acute lymphoblastic leukemia	CGH result from $BCL6^{+/+}$ and $BCL6^{-/-}$ BCR-ABL1 ALL	Supplemental Figure 12
GSE24493	Effect of Imatinib on chronic myelogenous leukemia (CML) cells	Gene expression result from human CML	Supplemental Figure 2a, Supplemental Figure 3